UNIVERSITÀ DEGLI STUDI DI ROMA "TOR VERGATA"

FACOLTA' DI INGEGNERIA

DOTTORATO DI RICERCA IN
INGEGNERIA DELLE TELECOMUNICAZIONI E MICROELETTRONICA

XXI CICLO

Design, processing and characterization of organic devices for optical communications

STEFANO PENNA

A.A. 2007/2008

Docenti Guida: Prof. Aldo Di Carlo, Ing. Andrea Reale

Coordinatore: Prof. Giuseppe Bianchi

a Tinozzino

Abstract

The recent explosion of broadband services and the limits imposed by the Moore's law have stimulated strong research activities towards the integrated optical chips, that are composed of a platform on which many different optical functions, typically in the C-band, are implemented. Such devices are particularly challenging because integration and compactness play fundamental roles. Among the different materials used to process the optical integrated devices, three main classes can be identified: semiconductors, glasses and organic materials. The last ones are particularly attractive because of the low cost of processing and the high integration related to the amorphous structure, resulting in not required lattice matching conditions.

A common design approach in integrated optics is to optimize a particular optical function with a specific material, then to integrate it on the platform. Among the functions to be implemented, amplification and light generation are still limited with respect to the other functions such as modulation or coupling/splitting. This is due to the limits imposed by erbium for the C-band operation. Indeed, erbium is difficult to be optically excited because of the small absorption cross section, so host sensitizers such as glasses are needed to efficiently collect the outer excitation and transfer it to the erbium ions. The most famous example of erbium sensitizer scheme

is provided by the Erbium Doped Fiber Amplifiers (EDFAs), wherein erbium ions are incorporated in glass matrices. However, EDFAs are not suitable for integrated chips since a long interaction length is required to achieve a sufficient gain level. Erbium-doped organic compounds are promising erbium sensitizers for the application to integrated chips as they exhibit attractive features such as high absorption and emission cross section, semiconducting behavior and low cost processing.

The aim of this work is to provide a demonstration of the potential of Er-doped compounds for the processing of an electrically driven integrated laser amplifier for the C-band of the optical communications. The different issues involved in such a challenging device have been studied separately, emphasizing the use of low cost techniques such as solution processing for organic deposition and LED pumping for the excitation of the active compounds. The opportunity for electrical pumping has been demonstrated with the processing of a spin-coated Er-doped organic LED. The optically pumped DFB cavities have been fabricated by nano-imprinting lithography and laser interference lithography and coated by Er-doped organic compound as active layer, resulting in a narrow emission line centered at 1530 nm. Finally, the waveguide issue has been addressed by designing a channel waveguide. Planar index discontinuity has been achieved by mean of a UV photo-patterning technique, purposed for the erbium-doped compound used in this work.

Contents

1. Introduction 1
1.1 Integrated Optics: state of the art 2
1.1.1 The Monolithic Approach 4
1.1.2 The Hybrid Approach 5
1.2 Erbium sensitizers 7
1.2.1 Ytterbium 9
1.2.2 Silicon 10
1.2.3 Silver ions 11
1.2.4 Organic compounds 12
2. Erbium doped organic thin films 17
2.1 Erbium tris(8-hydroxyquinoline) 19
2.1.1 Vacuum thermal evaporation 21
2.1.2 Solution 23
2.1.4 Spin-coating 27
2.1.5 Degradation 31
2.2 Enhancement of IR efficiency in Er-doped organics 32
2.2.1 Halogenation of 8-hydroxyquinoline in ErQ 33
2.2.2 Fully halogenation of Er-doped tetraphenylporphyrin 41
3. Organic Light Emitting Diodes for C-band 43
3.1 Working principle of an OLED 44
3.2 Design of ErQ-based OLEDs 46
3.3 Solution processing and fabrication 48
3.4 Characterization 50
3.5 $Na[Er(Q57Br)_4]$ based OLED 55
4. Organic DFB cavities for C-band 56

4.1 State of the art of organic resonant cavities 57
4.2 Design of a DFB cavity for C-band application 60
4.3 Processing 62
4.3.1 Grating fabrication 62
4.3.2 Evaporation of the active layer 64
4.4 Characterization 65
5. Erbium-doped organic channel waveguides 68
5.1 UV-exposure of ErQ thin films 69
5.2 ErQ Channel Waveguide 71
5.2.1 Design of the waveguide 71
5.2.2 BPM simulations 72
Appendix 77
Luminescence measurement systems 77
Conclusions 79
References 81
List of publications 89
Published Proceedings 89
Acknowledgements / Ringraziamenti 90

Chapter 1

Introduction

In the 1990's the worldwide explosion of Internet drastically changed the way people transfer information, allowing all computers on the planet earth to be connected to each other simultaneously. Beside to the sociological and romantic aspects, this meant a strong increase of demand for enhanced information capacities, due to the spreading of broadband services, and so an increase of cumulative demand for higher bandwidth. As a result, two consequences have followed: 1) fibre optics have become the pervasive technology not only for long haul but also for metropolitan communications, replacing the copper-based interconnects, and 2) new concepts of networking have been developed towards the all-optical processing of light, extending the use of fibre optics from the nodes to the home line terminations (Fibre To The Home, FTTH).

Therefore, a huge increase in the complexity of the optical systems has taken place, from point-to-point transmissions to the Wavelength Division Multiplexing (WDM)networking. The optical fibre is a medium with a extremely high bandwidth, about 20 THz, nevertheless today it is impossible to use a laser able to exploit this enormous bandwidth, so multiple single wavelengths laser signals can be multiplexed and transmitted on a single fibre. This is the working principle of WDM, developed in the mid 1990's. Dense WDM (DWDM) systems with more than 60 wavelengths, each

having 40 Gb/s data, have been demonstrated, so that the total transmission capacity of an SMF is higher than 2.5 Tb/s [1].

In terms of market, there has been a change of philosophy, from the ”bit rate distance product at any cost” challenge of the past [2] to a higher care for cost reduction of the technology in order to bring the optics closer to the customer, according to the FTTx concept. The bottleneck in the deployment of optical networks has always been the availability of low cost components suitable to large scale manufacturing. Unlike electronic components, optical connections needs a good light coupling between fibres and devices, otherwise optical power losses occur making the performances unacceptable.

Integrated optics is given to be the key to meet these requirements, allowing to handle the increased complexity of the WDM optical systems and keeping the cost of technology low in order to enable the massive implementation of FTTH.

1.1Integrated Optics: state of the art

There are many slightly different definitions for Integrated Optics (IO), but all of them agree on stating that a Photonic Integrated Circuit (PIC) is an opto-electronic device that implement all of the main optical functions on a single chip [3].Typically PICs operates at wavelengths in the visible and near infrared range, from 400 nm to 1650 nm.

Two basic issues must be considered in IO and put in evidence the big differences with integrated electronics: (1) the light in a PIC must be confined inside a waveguiding structure to enable propagation of the optical signal all along the chip and (2) the different functionalities must be integrated on the same device with the mandatory condition of low cost fabrication.

“While the electronics industry has been able to squeeze millions of devices onto tiny chips, the photonics industry has struggled to place a handful of devices onto a board! And while microelectronic engineers have been able to create complex systems at throwaway prices, most optical networking products still take the form of expensive point-to-point links.”

This statement is an excerpt of “The Market For Integrated Optical Products: 2001-2005” report from “Resources And Market” [4] and depicts the state of infancy of IO in terms of development and actual application with respect to the

corresponding electronic integration. This is partially due to the just recent interest of industries in exploration of the potentials of photonics, with the major companies traditionally focused more on pushing the limits of microelectronics than on developing efficient alternatives. The reason is just the intrinsic lower complexity: microelectronic integration technology allows for a broad class of electronic functionalities to be synthesized from a small set of elementary components, such as transistors, resistors and capacitors. Such a technology that supports integration of these elementary components can be used for many different applications and investments made in its development have a potential payback on a larger market [5]. The higher complexity for photonics lies in the variety of elementary devices: couplers, filters, MUX, lasers, detectors, switches, modulators, among the others, are all devices with different working principles each other and have been reported to be implemented with different materials and technologies, so that integration is a very hard target to be centred. Furthermore, passive integrated optical devices and optical interconnects are significantly larger than their electronic counterparts, so the photonic VLSI is impossible to achieve, at least with the current technological perspectives [6].

Anyway, in the last years a change has occurred, taking IO from the small hi-tech university spin-out companies (Luxtera, Optical Cross Links, Inplane Photonics) to the industrial applied research of the major companies (Intel, Enablence, DuPont, CyOptics, NeoPhotonics). This is due to the needs of the computing industry to keep the pace with the increasing processor performance, driven by the Moore's Law. So the need is for new solutions of optical interconnects for clock distribution first and for signal processing then. As a benefits, the material science and the technological mastery of design and fabrication of PICs has increased, leading to the definition of two main alternative approaches that differ for choice of materials and basic concepts to achieve the integration.

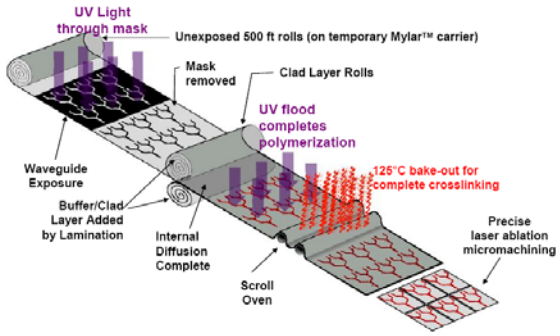

Figure 1.1. Volume manufacturing process of optical polymer waveguided circuits [7]

Beside to optical interconnects, a practical demonstration of the benefits coming from IO can be found in the WDM key-component, used for commercially available MUX/DMUX: the Arrayed Waveguide Grating (AWG). The AWGs are Photonic Integrated Circuits (PICs) typically formed on silicon substrate. They integrate multiple optical functions on a single substrate leading to a single package, volume manufacturable on a fab that is well developed in the semiconductor industry. Moreover, this technology allows integration of actives and passives on a single substrate leading to further size reduction, efficiency and reliability. An AWG optical chip is composed of input waveguides, an input slab, array of waveguides, output slab, and output waveguides. All of these are fabricated on a single substrate forming an optical integrated circuit. This device represents a deep improvement with respect to alternative solution for WDM MUX/DMUX such as Fibre Bragg gratings and cascaded filters [8].

Before description of the different IO technologies, it must be considered that in the IO area the transmission medium (polymer waveguide or silica fibre), the integration platform (silicon, GaAs, InP, polymer, silica) and the level of integration (monolithic opto-electronic, monolithic photonic integration with separate electronics, or optical platform with hybrid electronic and optical components) are still a matter of active investigation, so there is not yet a clearly pervasive technology, even if nowadays silicon photonics is able to gain higher funding from industry, thus assuring more resources for R&D.

1.1.1 The Monolithic Approach

The first approach aims to achieve the monolithic integration, implementing the optical functions with silicon. The attractiveness of silicon-based optics is the potential integration with CMOS integrated circuits for high-volume manufacturing. The first prototypes of such silicon-based optical components includes several basic functions on a single silicon chip, such as a thermally tunable WDM Bragg filters, high-speed optical MZI modulators and a Si/Ge high-speed photodiode [9] or a continuous-wave Raman silicon laser [10] that exploits the Stimulated Raman Scattering (SRS), in which sub-bandgap photons interact only with phonons. The last work, from people at Intel, is particularly impressive, even if it has not a practical use (optical excitation required, small spectral range of wavelengths for optical gain [11]), because achieving optical gain and/or lasing in silicon has always been one of the most challenging goals in silicon-based photonics: bulk silicon is an indirect bandgap semiconductor, resulting

in radiative (light emitting) decay being less likely compared to other non-radiative (e.g., Auger recombination) routes, and thus in a less-efficient corresponding light emission [12]. Furthermore, there is a mismatch between silicon band edge luminescence at 1100 nm and the requirement to operate at wavelengths around 1550 nm for full compatibility with fibre optic communications systems. So, light emission in silicon has traditionally focused on the use of silicon engineered materials such as doped nanocrystals [13], Si/SiO_2 superlattices, erbium-doped silicon-rich oxides [14], surface-textured bulk silicon and Si/SiGe quantum cascade structures [15]. The flaw of such a monolithic approach lies in the difficulty to implement all the optical functions meeting at the same the high performance expectations required.

1.1.2 The Hybrid Approach

A completely alternative approach is based on the consideration that, as previously noted, optical components such as tunable WDM filters, photodiodes, optical waveguides are all devices optimized with different materials and technologies, precluding them from an easy optoelectronic monolithic integration. Therefore, a valid method to achieve high performance at the lowest possible cost is the choice of the most appropriate material for each function on one side and the parallel development of an integration-friendly platform on the other side, resulting in a different method [3]. This is the so-called hybrid approach, that comprises also amorphous materials, such as polymers, that are free from restrictions related to the lattice matching condition of the crystalline structures.

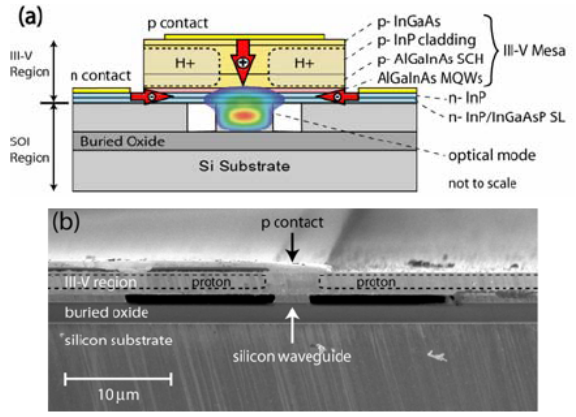

Figure 1.2. Device structure of a hybrid silicon evanescent PIC [15]

A first hybrid approach makes use of III-V compounds, commonly used for electroluminescence and lasing in the telecommunications windows, aligning and bonding pre-fabricated III-V active devices to individual waveguides fabricated on a silicon platform. This approach has the benefit of using electrically pumped active devices on a silicon platform, but since the III-V devices are aligned and bonded individually, the time and cost of manufacturing limits the total number of lasers that can be bonded on a single wafer. Moreover, limited alignment accuracy causes coupling loss variation and large reflection between the III-V active devices and the silicon waveguides. As alternative for III-V compounds, the device can be grown on silicon platform [16]. This approach is compatible to silicon and, moreover, allows for electrical stimulation, but the manufacturing procedures are complex and expensive, so the key requirement of low cost manufacturing can difficultly be met.

Many different optical technologies have been demonstrated including polymer waveguides integrated on Si, planar light wave circuit interconnects and fibre ribbon arrays integrated with VCSELs and photodiodes. Polymer waveguides are selected because of their potential for high-volume, low-cost production. For instance, the acrylate-based (PMMA) multimode polymer waveguides are known for their low loss (0.08 dB/cm), ease of integration, best system performance and manufacturability [17][18]. Polymers can be made photosensitive and as such can be directly photo-patterned and wet-etched with a solvent, speeding the fabrication cycle time to tens of minutes per multi-layer optical circuit on a wafer. These materials have an obvious throughput advantage in production [3]. Beside to waveguides, that today gain the most of interest from industry for the chip-to-chip interconnects, polymers and organic materials in general have been demonstrated to be efficient materials for several optical devices, like EO modulators [19], detectors [20] and amplifiers [21].

Other amorphous materials than organics are used for IO devices, like sol-gels, that are used for low cost processing of Bragg reflector waveguides, exploiting the UV-induced tuning of the sol-gel refractive index (over a range of 0.1) to obtain the proper index profile for light confinement [22]. In addition, sol-gel based IO devices integrating modulators, tunable filters and switches have been reported [23].

Doped glasses are another alternative solution for waveguided IO devices [25] that has already met the commercial availability, with some examples of Erbium Doped Waveguide Amplifiers (EDWAs) manufactured at Teem Photonics [24].

Finally, ceramic oxides like alumina (Al_2O_3) that incorporate active materials (see 1.2) have also been used for efficient waveguiding amplifiers [21].

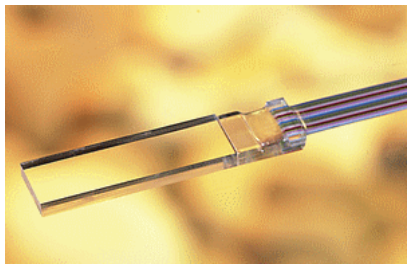

Figure 1.3. An Ion-Exchange planar glass waveguide from Teem Photonics [24]

1.2 Erbium sensitizers

One of the critical issues in IO is the need for compensation of loss, mainly due to absorption and scattering inside the device and to the light coupling among devices, that can make the performances unacceptable. So, a great interest is focused on the active materials and solutions that can be integrated on a waveguide. Furthermore, these active materials can be used for implementing the functions of signal generation and amplification on the integrated platform, mostly in the 2nd and 3rd optical communications standard windows, centred respectively at 1310 nm and 1550 nm. As previously mentioned, III-V compounds can be used to have light generation in these ranges, but they take disadvantages due to the expensive manufacturing technologies involved in III-V compound processing.

Therefore, a valid alternative is represented by some Lanthanide elements, the so-called Rare Earths (RE), whose optical transitions lie in the ranges of interest for IO, mainly Erbium, Neodymium and Ytterbium. To process a device entirely with such materials would be extremely expensive, hard from a technological point of view and finally inefficient because the optical transitions in the free ions are parity forbidden [26]. Nevertheless, these materials can be incorporated in host materials that can act as sensitizers. Erbium doped materials have attracted a big interest because of their unique emission properties ideal for IO, related to the $^4I_{13/2} \rightarrow {}^4I_{15/2}$ transition near 1540 nm wavelength that matches the lowest-loss window in optical fibre systems. The erbium trivalent ions (Er^{3+}), that is the favourite bonding state of erbium, shows an intra 4f shell transition from its first excited state $^4I_{13/2}$ to the ground state $^4I_{15/2}$ which results in the near infrared light emission at 1540 nm [27]. In the pure Er^{3+} ions this process is parity forbidden because the energy levels of the 4f shells have equal parity. However, if erbium is incorporated in a solid host, the transitions become weakly allowed because the wave functions of the electrons are in

some way “disturbed”. Because the transition is an atomic dipole, the absorption and emission cross section for the optical excitation are quite small ($\sim 10^{-21}$ cm^2) and the lifetimes of the luminescence are quite long, in the order of 1 ms [11][26][27][28]. Moreover, erbium ions in a solid are influenced by the electric field that removes the degeneracy of the 4*f* levels, resulting in a Stark-splitting of the energy levels, so that manifolds arise instead of sharp levels [29]. Due to the outer shell shielding, the magnitude of the splitting is small, resulting in relatively narrow lines of emission that are independent of the host material.

The most representative application of erbium in photonics is the Erbium Doped Fibre Amplifier (EDFA) [30] that is composed of a glass fibre whose core is doped with erbium ions. EDFAs can be efficiently optically pumped by a 980 nm or 1480 nm emitting laser to get the right population inversion. EDFAs are the current pervasive technology for optical line amplification. However, this technology presents some features that make it unsuitable for IO. First, the size: to get enough amplification, a long fibre cable is needed (typically in a 10 - 40 m range) because erbium concentration in the glass host is limited by quenching effects, such as ion-ion interactions, that convert the pump photons into heat. In addition, the issue of erbium clustering in silica must be considered since it is sensitive to composition and exacerbates the cooperative processes (cross relaxations and up-conversion) [31]. The other main flaw is the cost. An EDFA is an expensive device mostly because it requires an accurate high power pump laser (10-100 mW) [27] to excite efficiently the narrow lines of erbium absorption. So, EDFAs can’t meet the requirements for low-cost and compact devices of integrated photonics.

To avoid the use of lasers and reduce the interaction length of the active medium a different approach is required. Erbium sensitization can play an interesting role in this context for the realization of EDWAs (Erbium Doped Waveguided Amplifiers). A sensitizer coupled to an Er ion can absorb pump photons with a much larger than erbium cross section and then it can transfer the energy to Er. If the sensitizer has a broadband absorption spectrum it may be pumped by a broadband source such as a LED, much cheaper than a laser (from 2 to 3 orders of costs). In such a case, by choosing the proper pump wavelength, one of the limiting factor to gain in erbium doped materials, the Excited State Absorption (ESA) may also be avoided [27].

In this paragraph, a deeper discussion on the different schemes available for Erbium sensitization is presented, showing how the integration approaches are still valid at this level and allow for a wide choice of solutions with different performance and cost requirements.

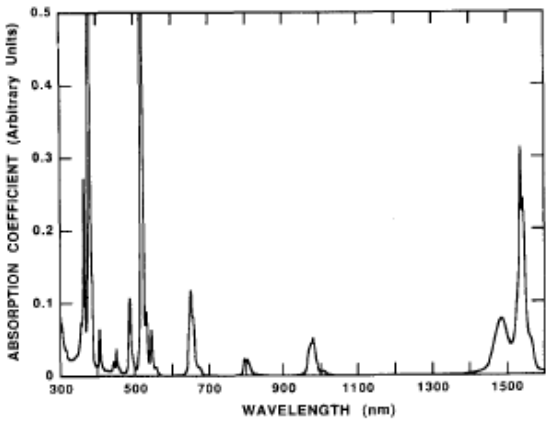

Figure 1.4. Absorption spectrum of Erbium doped silicate glass [31]

Currently there are four schemes available for erbium sensitization: (1) Ytterbium, (2) semiconductor (typically Silicon) nanocrystals and nanoclusters, (3) metal ions and (4) organolanthanide compounds.

1.2.1 Ytterbium

The ytterbium ion (Yb^{3+}) shows a 980 nm-peaked absorption band that is almost resonant with the erbium band $^4I_{13/2}$. The absorption band of Yb^{3+} at 980 nm is quite wide, thus Yb^{3+} can be excited by a broad band source in the range 850 nm – 980 nm. Since the absorption cross section of Yb^{3+} at 980 nm (10^{-20} cm^2) is tenfold the one of erbium, Yb^{3+} can efficiently absorb the pump radiation and transfer it to Er^{3+}, resulting in a several times more efficient excitation of Er^{3+} than the direct excitation of Er^{3+} [27]. In addition, ytterbium is a two-level system that is not affected by upconversion between the ions [32]. A disadvantage of such sensitization scheme lies in the reversibility of such a process due to the energy backtransfer from erbium to ytterbium. Another flaw is the limited concentration of Yb. Indeed, over a threshold limit that depends on the waveguide cross section, the upconversion coefficient and the ESA cross section, the ytterbium concentration is countereffective as it causes a poor improvement in gain with respect to the only Er doped waveguide, due to the effect of the large absorption of Yb [27].

Anyway ytterbium is currently often used as co-dopant for instance in Er^{-} doped polymer waveguide amplifiers [32] and Er-doped phosphate glasses [33] as it

contribute to enhance the effective pump-absorption cross section of Er^{3+} ions resulting in an improved photoluminescence efficiency.

1.2.2 Silicon

Bulk semiconductors are naturally efficient sensitizers for rare earth ions. When RE ions are incorporated inside a semiconductor, they act as point defects that introduce defect levels in the semiconductor bandgap, enabling the generation of traps for the optically or electrically induced carriers. The trapped carriers can generate a bound exciton and, according to the impurity Auger process, can recombine by energy transfer to the RE ions exploiting the strong spatial overlap. Like Yb^{3+}-Er^{3+} sensitization, in this case the process is reversible, too, with the quenching of the infrared emission of erbium due to the generation of an exciton induced by the strong exciton-Er coupling. The energy backtransfer has been proved to be highly effective at room temperature [34]. Indeed, erbium-doped silicon waveguides have shown infrared light emission when the silicon is co-doped with oxygen to produce optically active ions in the lattice [35]. A PN junction can be formed and the erbium ions can be pumped electrically to give electroluminescence [12]. Unfortunately, although emission can be relatively strong below 100 K, the emission intensity falls rapidly when the device is heated to room temperature [34].

A solution for such an undesired process is to increase the bandgap in the bulk silicon in order to make the backtransfer less probable on one side and to decrease the coupling erbium-excitons on the other side. To achieve the first target, the silicon bandgap can be enhanced by co-doping with oxygen [27] and processing the Silicon in such a way that Si nanocrystals [36] and/or nanoclusters [37] (Si-nc) generate within the silica matrices. The second target can be centered optimizing the Er-exciton coupling within the silica matrix that is dependent on the spatial separation between the nanocrystal and Er. Therefore, the coupling depends on the erbium concentration: typically, the higher the concentration , the lower is the nanocrystal luminescence, but at the same the lower the concentration, the lower is the Er-exciton backtransfer. It has been demonstrated that the proper level of erbium concentration is within a range of 0.02% - 0.04% weight [27].

These structures have showed many properties that make them optimum sensitizers. Indeed, silicon nano-crystals suspended in silicon-rich oxide restrict carrier movement while still allowing electrical pumping [38]. In terms of performances, the effective excitation cross section of the Er^{3+} 1.54 μm peaked luminescence broadens and strengthens up to values of 10^{-16} cm^2 under visible light pumping, with quantum

efficiencies greater than 60% by pumping at 488 nm. In addition to the increase of excitation cross section, Si-nc increase the average refractive index of the dielectrics, allowing good light confinement for waveguiding, and conduct electrical current, which enables the electrical pumping of optical amplifiers [37]. These structures are affected by strong detrimental phenomena such as cooperative upconversion and confined carrier absorption.

Recently, a LED pumped Er-doped nc-Si/SiO_2 silica micro-amplifier (amplet) has been reported [39]. This represents an important goal in the definition of low cost and compact waveguided devices for integrated photonics.

However, expensive and high consuming manufacturing techniques are involved in the processing of Silicon nano-particles, such like RF sputtering, ion implantation, aerosol synthesis, chemical vapour deposition and reactive evaporation of silicon rich oxides [11]. Indeed, high temperature thermal curing is required to form silicon nano-clusters (750 °C) and nano-crystals (1100 °C).

1.2.3 Silver ions

When incorporated in a glass, silver has been demonstrated to be a good sensitizer for erbium, since it has shown several absorption and emission bands in the visible and near ultraviolet ranges [27] that can be resonant with erbium manifolds.

Silver doping of glasses is commonly achieved by ion exchange, a cheap and well performing technique [40], wherein network modifiers of the glass such as Na^+, K^+ are interchanged with the silver ions [27]. In such a way a good index discontinuity can be obtained to process waveguides on glass substrate [41].

Recently, a single-end pumped waveguide laser based on Er:Yb-doped phosphate glass has been realized, showing an output power higher than 20 mW with a 17% efficiency at 1533.3 nm. Although their absorption cross section is low if compared to nc-Si (10^{-20} cm^2 for 980 nm pump band [42]), phosphate glasses can be heavily doped. For such a reason they are preferred to silica glasses wherein erbium concentration is limited by quenching effects in silica. Indeed, as previously mentioned, highly doped material is required to meet the demand of high-power together with a compact laser cavity (in the order of few cm). Furthermore, phosphate glass also makes co-doping with Yb^{3+} ions more beneficial for pumping in view of higher phonon energies in the phosphate, resulting in efficient energy transfer from Yb to Er [43].

In such a way, phosphate glasses allow to achieve higher efficiency of emission at 1550 nm, and so the interaction length of the device, particularly critical for integrated optics, can be reduced [44].

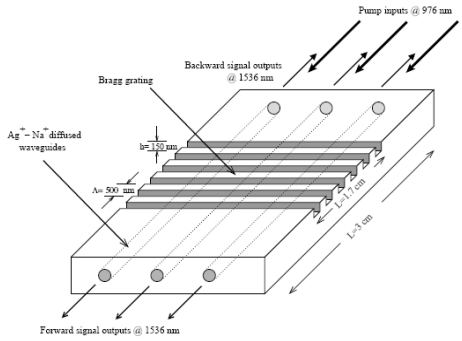

Figure 1.5. Layout of a laser chip fabricated on Er-Yb codoped glass substrate [41]

Nowadays, glass integrated optics seems to be a good compromise between semiconductor lasers and optical fibre lasers. Semiconductor lasers exhibit a high emission wavelength sensitivity to external noise sources such as temperature. On the other hand, optical fibre lasers show very good stability but are cumbersome, making integration extremely complicated. Furthermore, glass devices requires lower temperatures for vacuum thermal annealing (350°C) [27].

1.2.4 Organic compounds

Erbium doped organic compounds have gained attention because of their appealing features as low cost, ease of fabrication on a wide range of substrates, low dispersion and broad luminescence bands. Polymer amplifiers can be integrated into existing optical polymer devices already demonstrated (and in some cases, commercially available), such as switches [45][46], splitters [47] and MUX [48], with low coupling losses.

Furthermore, the opportunity of organic synthesis allows for “tailoring” of molecules, i.e. the engineering of the materials for the control of various optical parameters such as refractivity, birefringence, thermal stability, among the others, important to proper design and realize a waveguiding device.

As mentioned, polymers have the advantage to be deposited by low cost solution-processing techniques such as spin-coating in room temperature conditions. The subsequent thermal annealing rarely is higher than 200 °C. Indeed, temperatures higher than 110 °C can be detrimental for some organics like polymers.

Inorganic erbium compounds such as erbium salts (e.g. erbium chloride) cannot be used as rare-earth sources in polymer matrix as they cannot be solvated by organic solvents. However, Er ions can be incorporated in an organic ligand to form an organolanthanide molecule that can be easily dispersed in a polymer film such as poly(methyl-methacrylate) (PMMA) [49] or poly(phenyl-methacrylate) (PPMA) [50] and in sol-gels [51][52]. In addition, the polymer matrix can act as sensitizer of the ligand, enabling a double steps excitation mechanism, as suggested in [50]. This ligand must provide enough coordination sites in order to bond to the erbium ion in a stable complex [27] and to shield the ion from the neighbours and from impurities in the polymer matrix that may quench the near IR fluorescence.

In organolanthanide complexes erbium can be directly excited, nevertheless the great advantage is that organic can be excited, too, resulting in a several times more efficient excitation. Indeed, the organic ligand acts as sensitizer for erbium, according to the Antenna effect [53] showed in Figure 6 and described here in the following.

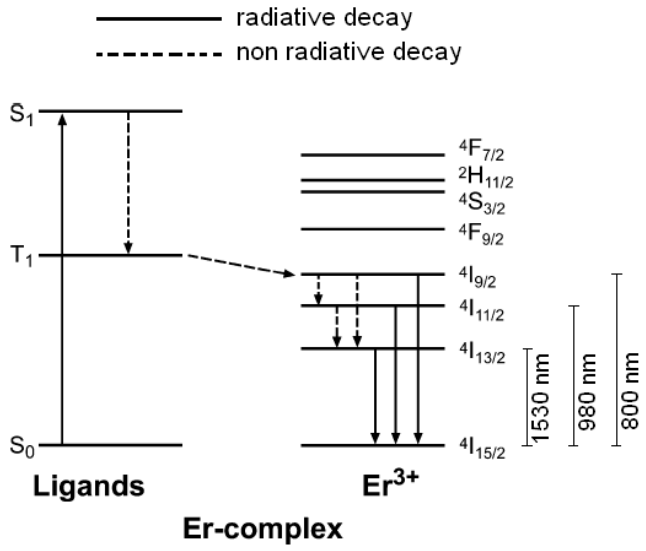

Figure 1.6. The Antenna effect in an organo-erbium system

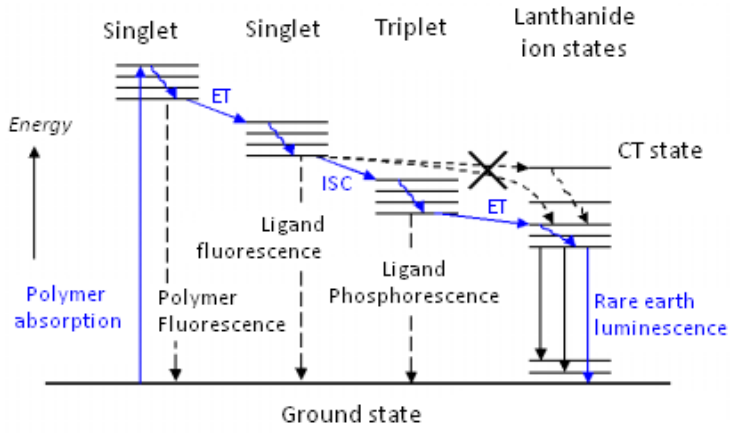

Figure 1.7. Sensitization scheme and energy transfers of an organolanthanide guest in a polymer matrix [54]

Typically, the organic complex acts as an "energy antenna", being efficiently excited from the singlet S_0 ground state to the singlet S_1 excited state. This is followed by fast relaxation to the triplet T_1 state and from there energy transfer to one of the Er^{3+} 4*f* levels may take place. From these levels, rapid relaxation to the $^4I_{13/2}$ first excited state in Er^{3+} takes place. Finally, the Er^{3+} may decay to the $^4I_{15/2}$ ground manifold resulting in the emission of a 1530 nm photon [27].

Er^{3+} ions in the organic complex have been reported to have an absorption cross section in the order of 10^{-20} cm^2, one order higher than the free Er^{3+} ions [27]. Unfortunately, short lifetimes (in the order of 100 ns) of luminescence have been observed, likely due to the quenching effect of water residuals within the molecule that coordinate with erbium [27][55]. It is known that OH groups are detrimental for near infrared absorption around 1420 nm, corresponding to the first vibrational overtone of the OH bounds. For instance, this led to the definition of the 2nd and the 3rd windows of telecommunications, just around the O-H related absorption peak in the silica fibres. For erbium ions, which exhibits a strong interaction with water, the same occurs, since the overtones of the OH groups positioned close to the erbium ion (1 nm) are resonant with the $^4I_{13/2} \rightarrow {}^4I_{15/2}$ transition [27].

Therefore, the short luminescence lifetimes requires for high pump power to get the proper population inversion. This flaw can be compensate by the high absorption cross section showed by the aromatic component of the organic ligand, whose value is in the order of 10^{-18} - 10^{-17} cm^2. The wide absorption band of the ligand typically lies in the ultraviolet range, with some cases reported in the near UV [56]. In this last case, the use of wide emission sources such like LEDs as pump sources is enabled, as shown in the next chapter.

With respect to infrared luminescence spectra observed for erbium coupled to the other sensitizers, the erbium-doped organic compounds show much wider spectra, with a spectral width (FWHM) of up to 80 nm [57]. The huge broadening of IR luminescence can be assigned to the coupling of the vibrational modes of the organic ligand with the 4f-4f electronic transitions of erbium, as expected [49]. This feature candidates such compounds as active materials for optical amplification, mainly in the C-band (1530 nm-1565 nm), but also in the neighbor S-band (1460 nm – 1530 nm) and L-band (1565 nm – 1625 nm). Furthermore, broad spectrum sources induce a lower ESA on the erbium ion, resulting in a better quantum efficiency [27].

The basic quantum yield of organolanthanides is low, in the order of 10^{-4} [50]. Besides to the previously mentioned OH group quenching, these low efficiencies are also associated with the high-frequency CH vibrational bands of the organic ligands that couple with the Er^{3+}, reducing the lifetime of the emitting level by multiphonon relaxation at microseconds, whereas it should be 3 orders of magnitude higher (4 ms). In order to achieve more efficient luminescence from lanthanides, and thus a higher quantum yield, it is necessary to complex the ions with a ligand functionalized by a chromophore that optimize the energy harvesting, in some cases shifting the absorption peak in the visible range of wavelengths, wherein cheaper and commercially available sources are available [50][57]. In such a away, 10^{-3} efficiencies can be achieved [50]. Recently, a erbium thiolate $(DME)_2Er(SC_6F_5)_3$ has been demonstrated [58] to give 75% efficiency with luminescence lifetime of 2.88 s, very close to the 4 ms upper limit identified for erbium-doped organic compounds [27]. This impressively huge efficiency is attributed to the absence of direct Er coordination with fluorescence quenching vibrational groups such as hydrocarbon and bonding of hydroxide groups. Indeed, there are no OH functionalities, and the limited number of ligands with CH bonds are connected to the Ln through weak dative interactions, rather than covalent bonds between the metal cation and a hydrocarbon chain or hydroxide ion. In both complexes, Er ions are bound to heavy elements such as S, Se, I, and fluorinated thiolates, and because of the proximity of such heavy elements and fluorinated organic functionalities, high fluorescence quantum efficiency is achieved.

Up today, the most popular erbium-doped organic complexes, that have provided good results when used in devices, are: erbium-tetraphenylporphyrin (ErTpp)acac that has been demonstrated to be efficiently dispersed in several polymers like MEH-PPV [57] and poly(arylene–ethynylene) (PAE) [58] to give electroluminescence, Er-doped polydentate hemisperands that have been reported to be used for polymer waveguiding amplifiers as dispersed particles in PPMA [27][50], whereas tris(dibenzoylmethanato)(monobathophenanthroline) erbium(III) complex

$[Er(DBM)_3]$ [59], erbium tris 8-hydroxyquinoline (ErQ_3) [60], erbium (III) 2, 4-pentanedionate ($Er(acac)_3$) [61] and tris(acetylacetonato)(1,10-phenanthroline) erbium $[Er(acac)_3(phen)]$ [62] have been reported to be used as active layers in electrically stimulated Organic Light Emitting Diodes (OLEDs), as it will be shown in the chapter 3.

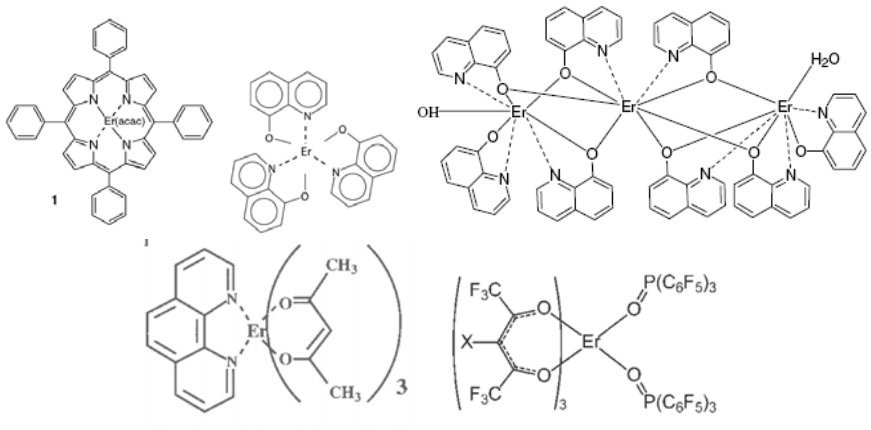

Figure 1.8. Some erbium-doped organic molecules [56][57][58][59]

Chapter 2

Erbium doped organic thin films

Thin film deposition of organic materials is a basic step in the processing of organic devices because a careful control on the thickness and the quality of the organic layer must be performed. Indeed, charge transport between molecules and exciton generation and recombination are mechanisms that are strongly affected by the presence of undesired impurities or not ordered roughness in an organic active layer. The low thickness values involved, in the order of 10 nm up to 100 nm, make the process control a critical issue.

Depending on the type of organic material, different deposition techniques are used. Small molecules, i.e. monomers or oligomers, that are light molecules with strong bounds and high melting point, are typically deposited by vacuum processing techniques, mainly vacuum thermal evaporation, which involves high temperatures (200 °C – 300 °C). Polymers, that are heavy molecules made of long chains of monomers, usually cannot be processed at temperatures higher than 110 °C as degradate before melting, losing the properties they are synthesized to. However, polymers can be easily solvated in solutions and deposited by room temperature solution processing techniques such as spray-coating, spin-coating or ink-jet printing. Then, thermal annealing at the boiling temperatures of the solvents, lower than 110 °C for most of organic solvents, is performed. Although vacuum thermal evaporation allows for a more controlled, accurate and impurity-free deposition, solution processing represents the key factor for the success of polymers in optics and

electronics because fast, simple and extremely cheap processing, mostly with respect to semiconductor's industrial techniques, can be used [3], meeting the requirements of the integrated optics for low cost, as mentioned in the former chapter.

Erbium-doped organolanthanides are small molecules, so they are naturally compatible to vacuum thermal evaporation. Nevertheless, in order to exploit the edges of solution processing, big efforts have been made to make these molecules easily and efficiently dispersed in polymer matrices to get a guest-host system [29][57].

In this work two types of erbium doped organic materials, erbium tris(8-hydroxyquinoline) [ErQ] and Er-tetraphenylporphyrin acetylacetonato [$Er(TPP)_{acac}$] has been mainly studied. Nowadays ErQ is the most appealing organic IR emitter because it has been demonstrated to be electrically stimulated to give IR electroluminescence from an OLED [63]. In addition, opportunity for dispersion in mesoporous silica [51] has been reported. Therefore, since few years ErQ is the only commercially available organo-erbium compound (Sigma Aldrich, Gelest, ABCR).

In order to exploit both solution processing advantages and ErQ benefits for 1550 nm emission, in this work a great effort has been made to solvate the ErQ and deposit it by controlled spin-coating. To evaluate the effects of the different deposition techniques on the ErQ optical properties (absorption and luminescence), thermal evaporation of ErQ has been performed and optimized.

This chapter presents the results related to the evaporation and the purposed spin-coating technique, developed to achieve a good quality deposition of ErQ thin films with 40 nm – 60 nm thickness. The same technique has been used to process an enhanced version of $Er(TPP)_{acac}$ thin films. Results of optical characterization of the solutions and the thin films is reported.

Finally, in order to reduce the C-H bonds-related quenching of IR emission and improve the quality of solution processing, halogenation of the two materials has been performed. Results on effects and improvements of such a study are reported in the end of the chapter.

It should be noted that ErQ has been optically characterized in form of powder, solution, drop-cast film, evaporated thin film and spin-coated thin film. This characterization has been aimed to verify possible variations of the optical properties depending on the state and the deposition technique used for the material. Absorption spectra have been detected with a Varian Cary 50 UV-vis spectrophotometer in a quartz cuvette. Luminescence has been detected by the spectroscopy set-up reported in Appendix A.

2.1 Erbium tris(8-hydroxyquinoline)

Erbium tris(8-hydroxyquinoline) (ErQ, CAS number 23696-16-8, formula $C_{27}H_{18}ErN_3O_3$), also named as tris(8-hydroxyquinolinato) erbium (III), is an organolanthanide molecule composed of three Quinoline groups coordinated to a trivalent erbium ion Er^{3+} (see Fig. 2.1). Recently, a trinuclear structure Er_3Q_9has been proposed [64], in which the Er metals are fully coordinated by the quinolinolate(Q) ligand molecules.

Besides to be an efficient sensitizer for erbium, Quinoline is also a popular organic semiconductor [4], used for charge transport properties in other organo-metal compounds such like Aluminum Quinoline (AlQ_3) that is commonly used as electron transport layer and green emitter in OLEDs [65].

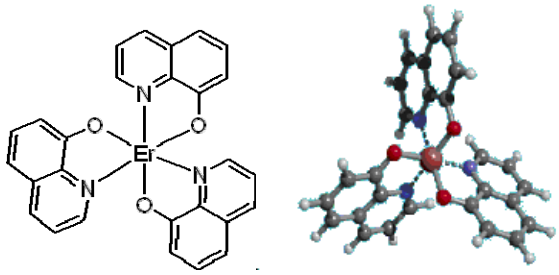

Figure 2.1. 2D and 3D pictures of an ErQ molecule

The sensitization scheme of ErQ accords to the Antenna effect resumed in figure 2.2 that also shows the energy values involved in the process: (1) absorption of a photon induces an excited singlet state on the Quinoline, (2) intersystem crossing from the excited singlet state to a triplet state, enhanced by the heavy atom effect, may occur, (3) intra-molecular energy transfer from the triplet state of the ligand to one of the excited 4f states of the lanthanide ion via a Dexter transfer mechanism takes place and finally (4) intra-4f transitions within the Er^{3+} produce IR luminescence. It must be observed that, differently from other rare earth quinolines wherein the triplet decay is strongly dominated by radiative decay (phosphorescence) with a characteristic visible emission at 600 nm, in ErQ the triplet decay is dominated by energy transfer to energetically resonant states of the erbium ion, mainly $^4F_{9/2}$ as reported by many study on the subject [66][67], as suggested by the spectral overlap between Er^{3+} absorption and the ligand emission reported in [68].

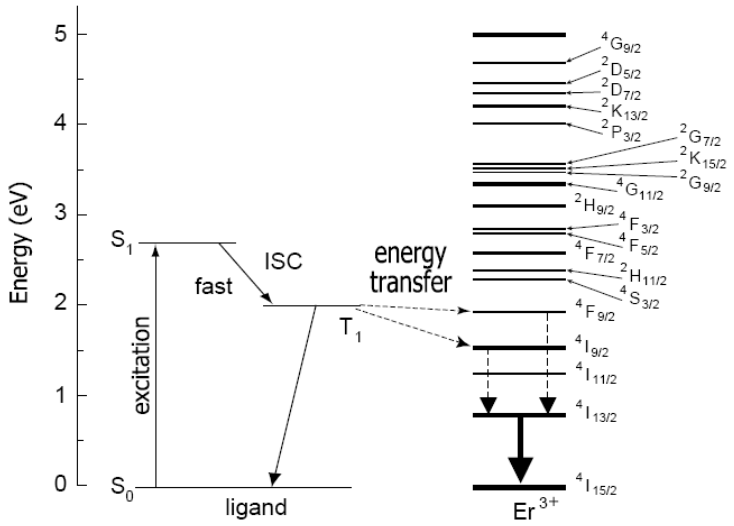

Figure 2.2. Sensitization and photoluminescence scheme of ErQ [69]

A typical absorption spectrum of ErQ is shown in figure 2.3, with a near ultraviolet (NUV) peak at 380 nm and a second lower peak at 325 nm. As previously mentioned, these peaks are related to the Quinoline that efficiently harvests the light excitation. This is consistent with what reported in previous publications [66], with the 380 centered band having a great spectral portion in the visible range. This band represents one of the big edge of this compound, since it enables the excitation by commercially available visible sources, as reported in [56]. The 325 nm secondary peak has been attributed to a vibronic progression due to the ring deformation modes [70].

Luminescence measured on ErQ powder in figure 2.4 showed the typical emission of the 4*f*-4*f* transition at 1535 nm. The spectral width (FWHM) value is 80 nm, from 1490 nm to 1570 nm. This is a much higher value than what reported in other erbium doped hosts, as discussed earlier.

The ErQ used for experiments has been selected from three different batches: a first batch from a lab-made powder coming from Queen Mary University of London (Dept. of Physics, Prof. W. P. Gillin), a second one from Gelest Inc. (purity > 95%, product number AKE276), a third batch from Sigma-Aldrich (purity > 97%, product number 658502). A common behavior in terms of absorption and infrared emission has been observed, instead the visible emission has been observed to be different in some cases, as it is reported in the following sections.

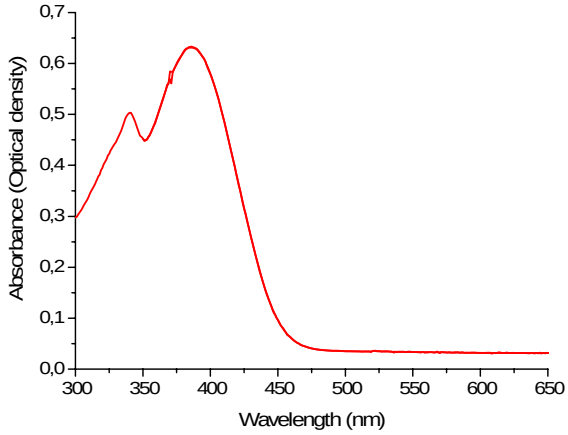

Figure 2.3. UV-Vis Absorption spectrum of ErQ powder

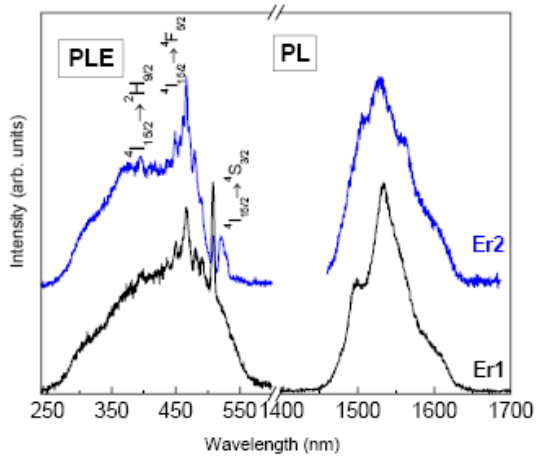

Figure 2.4. Excitation (PLE) and IR emission (PL) spectra of ErQ powder
(ErQ is identified as Er1)

2.1.1 Vacuum thermal evaporation

Vacuum Thermal Evaporation (VTE) is the basic deposition technique for small molecules such as ErQ that exhibit a melting point at temperatures lower than degradation point, thus tolerating the high temperature involved in the process. ErQ has a melting point floating from 280 °C to over 300 °C as reported by producers [Sigma Aldrich, Gelest]. However, evaporation of uniform thin films is not an easy task

to complete, nor evaporation parameters of the material, such as weight density and Z-ratio, are known. Therefore, several tries have experimented to control and optimize the process. Evaporations have been performed with a on borosilicate glass and silicon dioxide substrates, enabling the spinning of the sample-holder to achieve a more uniform deposition. It has been found that selecting evaporation parameters as in the following:

- weight density: 1.55 g/cubic cm
- z-ratio: 1
- tooling: 200 (specific for evaporation system)
- chamber pressure before evaporation: 7.4 x 10^{-7} mbar

In such a way an accurate control has been achieved with a typical mismatch between the nominal and actual thickness values in the order of 0.3%. Figure 2.5 shows the step of the thin film on the substrate: the missing of particles on the layer emphasizes the quality of the process.

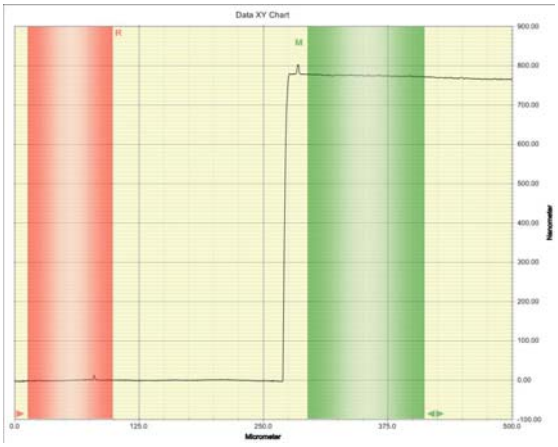

Figure 2.5. Surface profile of ErQ thin film (780 nm) on Silicon (100) wafer

Optical characterization performed on the evaporated thin films in the visible range, showed in figure 2.6, resulted in a 525 nm centered spectrum that is consistent with previous publications [63][68]. This peak is related to the ligand singlet emission. Typically, in many lanthanide-quinolinate compounds such as YbQ a 600 nm peak is also observed, related to the triplet radiative emission. The absence of this peak in ErQ demonstrates the efficiency of the triplet-to-ion energy transfer, that dominates on the radiative deactivation of the triplet [68].

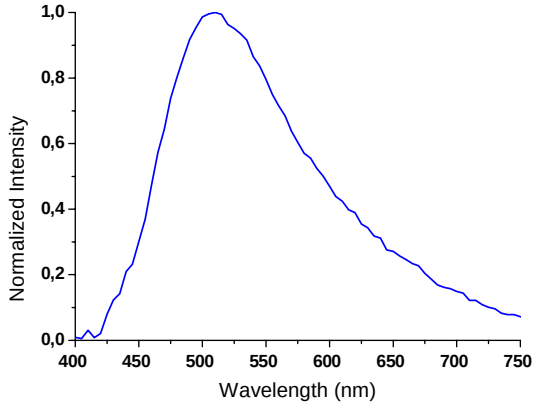

Figure 2.6. Visible photoluminescence of an ErQ thin film deposited by VTE

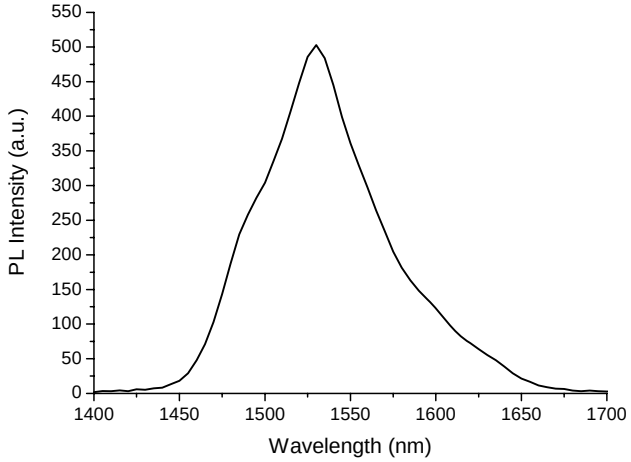

Figure 2.7. IR photoluminescence of an ErQ thin film deposited by VTE

The infrared luminescence spectrum in figure 2.7 showed the typical erbium-related 1535 nm peak. The side peak at 1490 nm is due to the side emissions of the $^4I_{13/2}$ manifold as an effect of the Stark splitting [55].

2.1.2 Solution

Although several publications [71][72] and producers [Gelest] report about ErQ as dissolvable in common solvents such like methanol and chloroform, it has not

been confirmed by direct experience. Instead, Dimethyl Sulfoxide (DMSO) and Dimethylformamide (DMF) have been experimented to be the only effective solvents on ErQ. For safety, DMSO has been selected as working solvent.

To allow for the spin-coating deposition of a layer as thicker as possible, the limit concentration of ErQ in DMSO has been searched for. The limit, identified as the threshold which the solution turns to opaque over, has been found to be 4% weight.

Figure 2.8. ErQ solution in DMSO at 4 % weight

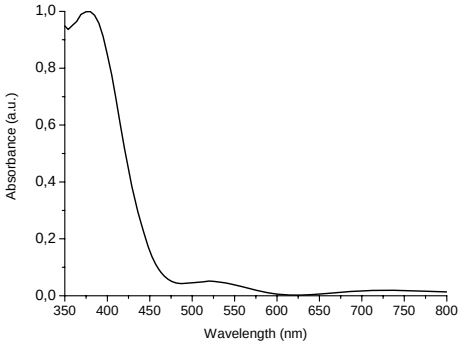

Figure 2.9. UV-Vis Absorption of ErQ solution in DMSO

Absorption characterization performed on ErQ solution in a quartz cuvette gave a spectrum (see figure 2.9) with a peak at 520 nm that can be related to the $4f^{11}$ manifold in the erbium ion (population of the $^2H_{11/2}$ level) [67][73], besides to the known peak of the ligand at 380 nm.

As previously mentioned, the visible luminescence shown in Fig. 2.10 strictly depends on the batch of material under characterization. In particular, the lab-made batch (in figure, ErQ batch) has the typical peak related to the singlet emission, even if slightly red shifted at 565 nm with respect to the usual ErQ emission at 525 nm. Furthermore, a 595 nm side peak can be observed. The solution based on the

commercial compound instead features an unexpected behaviour with two peaks at 618 nm and 664 nm, that are reported for ErQ powder [72] and the ErQ-based evaporated OLED by Gillin [63]. Emission at 600 nm is associated to triplet emission in Quinoline [66], but it has never been observed in ErQ because most of triplet decay is routed towards energy transfer to erbium resonant manifolds rather than towards phosphorescence (triplet emission). It should be noted that in the evaporated thin film, for both the batches, only the 500 nm peak can be observed, as reported in figure 2.11 for a comparison, so the unexpected emission of Gelest compound could be explained by effects of the DMSO on the molecule.

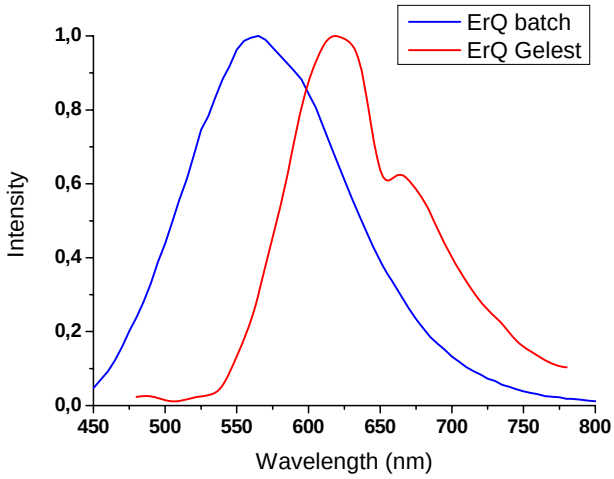

Figure 2.10. Visible luminescence of ErQ solution in DMSO at 4 % weight

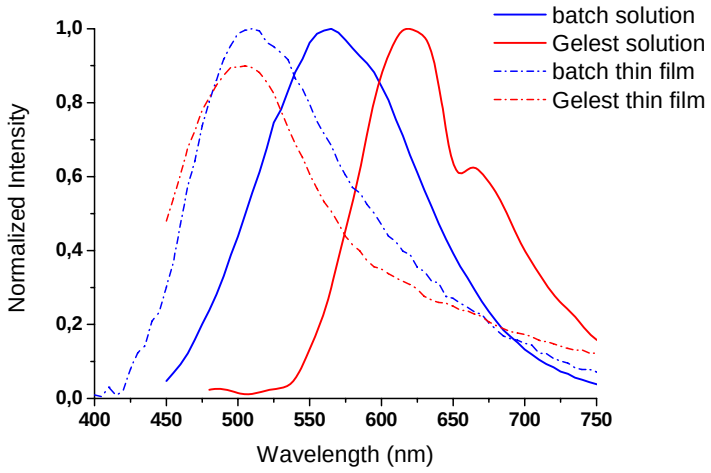

Figure 2.11. Comparison of visible luminescence of ErQ solution in DMSO (4 % weight) and evaporated thin films for two batches of ErQ

A possible further explanation could be found in the low purity of the commercial ErQ powder, 95% for Gelest batch, whereas lab-made batch is supposed to have an higher degree of purity (typically 99,99%), but it is not enough to explain the absence of the traditional singlet emission in the green range.

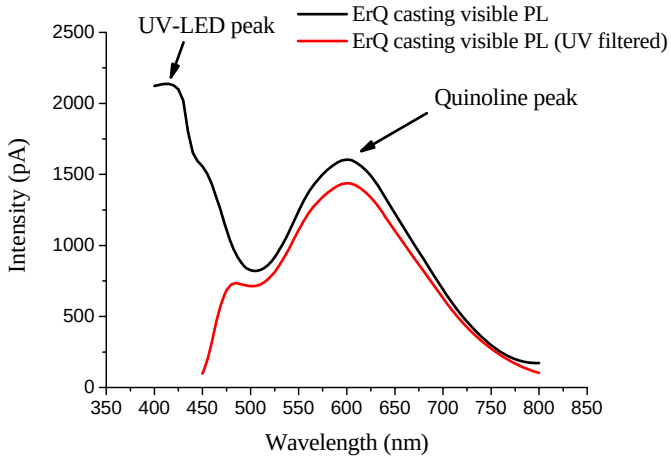

Figure 2.12. Visible luminescence of drop cast sample from ErQ solution (DMSO, 4 % weight)

The 600 nm visible peak has been observed in the drop cast sample of the Gelest batch, too, after thermal curing at 190 °C to completely remove the solvent residuals form the layer. An UV-LED has been used as excitation source. This result suggests the interaction of the solvent with the compound as a possible explanation of the different behavior between the evaporated thin film and the ErQ solution.

Infrared emission is not affected by different batches, showing the expected characteristics both for solution and for drop cast sample. In Fig. 2.13 it is possible to observe all the IR transitions of erbium in the organic molecule, confirmed by previous works [63][67].

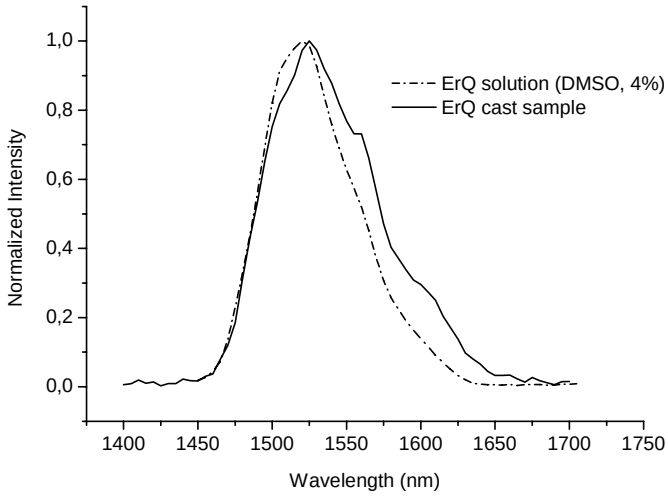

Figure 2.13. IR luminescence of the ErQ solution (DMSO, 4 % weight) and the related drop cast sample

2.1.4 Spin-coating

Spin-coating is the basic deposition technique for solution processing. Usually it is performed at room temperature conditions as the spinning is sufficient to produce the uniform spreading of the solution and the complete boiling of the solvent. Nevertheless, for what it has been directly experimented, ErQ can be solvated only in Dimethyl Sulfoxide (DMSO), a high boiling point (189 °C) solvent that makes the traditional spin-coating not effective, as it can be observed in the figure 2.14, resulting in a non-uniform thin layers. This is due to the high polarity of DSMO

that makes the solution really viscous, so that drops are generated from the spinning action (see the spots of the sample the figure 2.14 (b)).

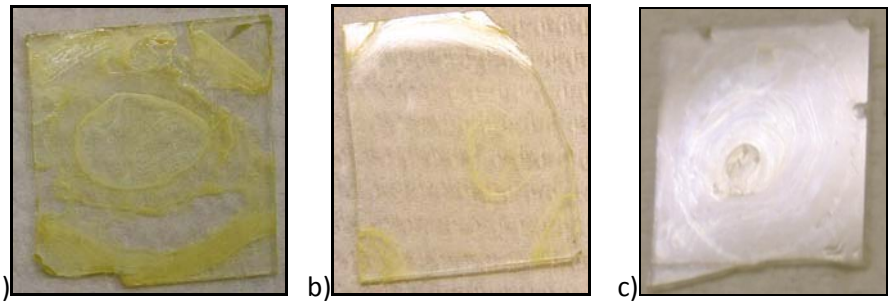

Figure 2.14. ErQ spin-coated films resulting from (a) 400 rpm, (b) 600 rpm and (c) 900 rpm

Therefore, it has been necessary to develop a purposed method that allowed for a better quality of deposition. Since the choice of solvents is limited to DMSO, a study has been made on the method to decrease the polarity of the solvent allowing for a uniform spreading of the solution all over the substrate during the spinning step. High temperature Spin-Coating (HTSC) [56] has been tweaked, involving a heat source over the sample to be used during the process. Optimization of the deposition has been achieved following the next procedure (for a ErQ in DMSO 4% weight solution):

1) Deposition of the solution onto the sample;
2) Heating on at 25 °C, sample not spinning;
3) Step 1 spinning at 500 rpm for 20 seconds to allow for a uniform spreading;
4) Step 2 spinning at desired speed to control the final thickness of the layer.

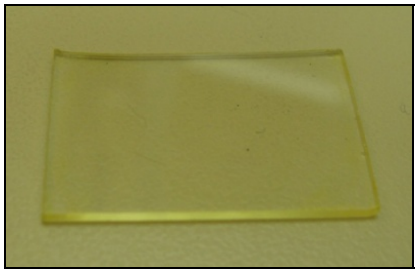

Figure 2.15. ErQ films resulting from high temperature spin-coating

The thin films obtained in such a way are showed in the picture in figure 2.15. It is possible to observe the improved quality with respect to the traditionally spin-coated samples in Fig. 2.14.

The HTSC technique has been calibrated to control the thickness of the layer. As shown in the figure 2.16 and 2.17 related to ErQ spin-coated borosilicate glass substrates, the IR luminescence of the ErQ coated samples has a linear dependence of the emission peak on the thickness of the layer, as expected [56].

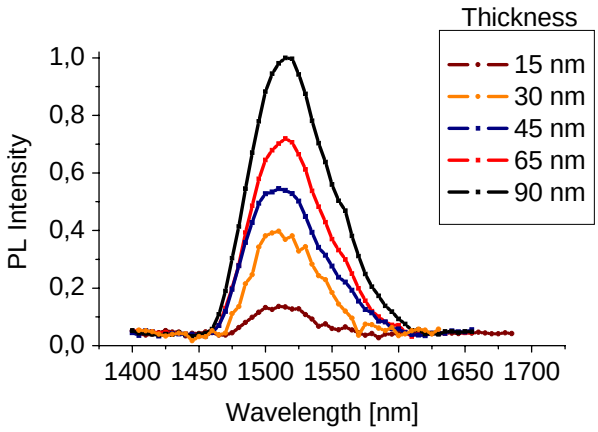

Figure 2.16. IR luminescence of ErQ spin-coated samples [56]

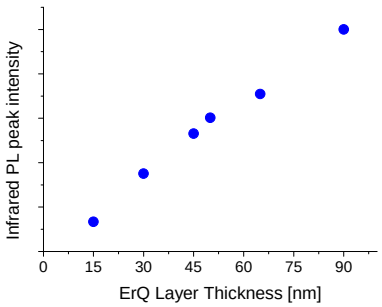

Figure 2.17. Linear dependence of 1535 nm peak on the thickness of the ErQ layer [56]

The IR luminescence from the samples has been induced both by laser at 406 nm and by a UV-LED peaking at 402 nm. The aim of this measurement has been to provide a practical demonstration of the benefits coming from the Er-doped organic compounds such as the potential for extremely low cost pumping, exploting the high absorption cross section and the broad absorption band of the ligand in the organo-metal. From a comparison between the laser-induced IR emission and the LED-

induced one (see Fig. 2.18), normalized on the optical power density incident on the spin-coated sample (38 mW/ 100 μm^2 for the laser, 380 μW/ 100 μm^2 for the LED), the same emission efficiency can be observed.

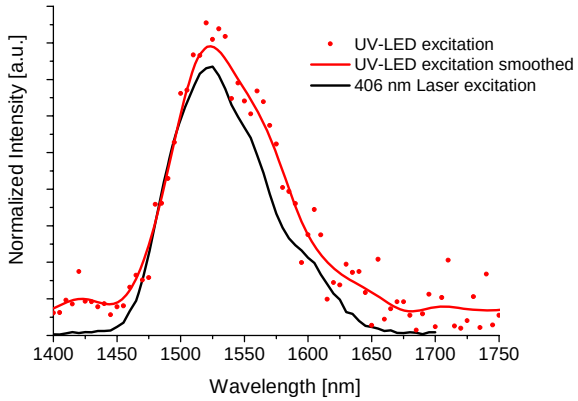

Fig. 2.18. IR emission of ErQ spin-coated samples (70 nm)

On summary, the Erbium related emission is not affected by the different deposition techniques, as shown in Fig. 2.19. This represents a good feature of ErQ as it enables the choice of the technique with the most suitable features to each device to be processed, as it is shown in the next chapters. In addition, it must be considered that measurements have been performed at room temperature. The demonstrated availability of spin-coating and LED pumping to achieve C-band emission are key elements in the processing of IO device as they allow for real low-cost applications.

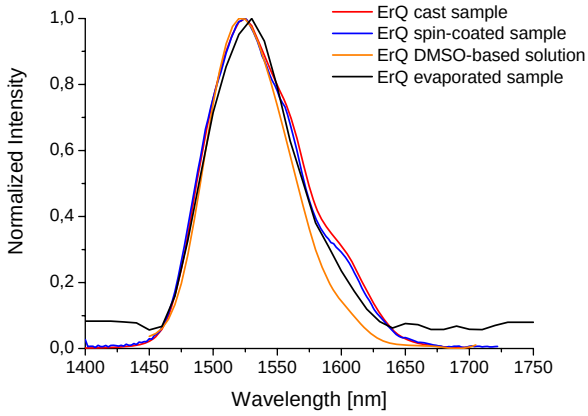

Fig. 2.19. IR emission of different ErQ samples

2.1.5 Degradation

The main flaw of the organic compounds in electronics and photonics is the fast degradation that leads to decrease the level of performance of a material making it not useful for a practical application. There are many causes for degradation. The first is the action of contamination of air, wherein moisture and oxygen can bound to the organic ligand resulting in an altered structure than the original. This is particularly detrimental for polymers, that offer many free coordination sites for contaminants to bound. Encapsulation and sealing are typical remedies to avoid or at least reduce the effect of air on the organic. Therefore, the ErQ samples have been encapsulated to measure the lifetime of the material under working conditions.

Dupont Surlyn 60 has been used to seal a borosilicate glass slide on a ErQ drop cast borosilicate glass substrate in a nitrogen atmosphere (glove-box). Laser-induced visible luminescence has been observed. The choice of visible range rather than IR range for observation is motivated by the working scheme of the molecule. Indeed, it is known that the organic ligand is the main photon absorbing agent and the fastest to exhibit degradation, as discussed above, so the singlet emission intensity is a meaningful parameter to evaluate the overall degradation. The results of this observation give a 50% decreasing on the visible peak at 550 nm in 60 minutes, even though the preliminary encapsulation. An exponential decay trend is observed in the decrease. The explanation for such a phenomenon can be found in the effects of optical pumping on the molecule, i.e. the so-called “laser annealing”. This means that the molecule degrades by simply working, as it is not stable enough to keep its original structure and properties. This is confirmed by effects on refractivity of the ErQ thin films induced by exposure to absorption peak light, as shown in the last chapter.

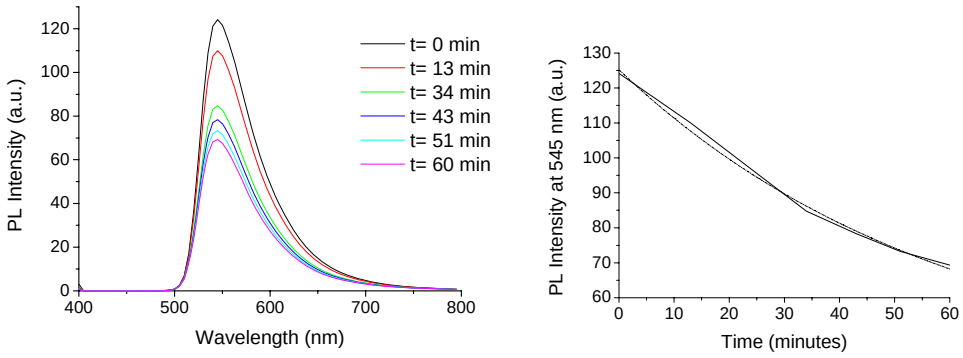

Figure 2.20. Degradation of the visible emission of an encapsulated ErQ film on glass substrate

2.2 Enhancement of IR efficiency in Er-doped organics

In the previous sections it has already been discussed about the quenching of 1535 nm-emission in the erbium-doped organic compounds. Indeed, because of the relatively small energy gap between the excited state $^4I_{13/2}$ and the ground state $^4I_{15/2}$ in the Er^{3+} ion, the triplet excited state is efficiently quenched by the vibronic coupling with high energy O–H, N–H or C–H stretching vibrations in the neighbourhood of the ion [73] [74]. This phenomenon reduce the energy transfer to the erbium ion resulting in a short luminescence lifetime (some microseconds), thus in a low emission efficiency (10^{-4}). IR quenching affects the most of the organic complexes, polymers too. Moreover, conventional polymer waveguides, that have been said to be extremely interesting for IO issues in chapter 1, tend to exhibit high optical propagation losses, due to absorption of infrared light at specific frequencies associated with the same overtones of C–H and O–H bond vibrations, limiting their potential for use in telecoms applications.

To address these issues and make polymer waveguides a practical alternative for integrated optics, minimization of such loss processes is pursued, usually by replacement of the hydrogen atoms with heavier atoms via deuteration or fluorination of the polymer host material, in order to shift the frequencies of the relevant vibrational overtones to less detrimental ranges [74].

So, one of the role of Er-doped compounds incorporated in such polymers can be the compensation of the propagation losses. The ligand in an Er-doped compound must meet several requirements to accomplish this task. (1) It must exhibit efficient light harvesting properties, also (2) it must protect lanthanide ions from the local environment by acting as a physical buffer. This shielding effect considerably reduces non-radiative de-activation processes arising from coupling with lattice, residual water (O–H bond) or solvent molecule vibrations. In addition, (3) the complete coordination of the ion by the ligand avoids the clustering phenomenon, consisting in ion-ion interactions that lead to quench the lifetime of the metastable state. This is due to the need of the erbium ion to complete its valence, thus clustering with another ion. To fully understand the potential of such issue, it must be considered that clustering is one of the main causes of limited Er^{3+} concentration in doped silica glasses (0.1 wt%). (4) Maximization of the energy transfer from the excited singlet state S_1 to the lanthanide is another requirement. Competitive with this process are mechanisms of fluorescence, phosphorescence and thermal decay to S_0. In order to maximize energy transfer to the central ion, the energy difference between the ligand chromophore triplet state and the excited energy level of the metal ion should not be

too large, with excited triplet state being of higher energy. A too small energy gap however will lead to back energy transfer from the lanthanide ion. Finally, (5) the quenching effects of C-H, N-H and O-H bonds must be cancelled or at least reduced.

Saturation of Er ion is the main strategy to design and synthesize a ligand that can meet these requirements. There are two complementary strategies to achieve that. One is focused on the saturation of the ion via organic cage-type structures [50] or using a macrocycle bearing a 8-hydroxyquinoline as light harvesting antenna as in [75]. In such a way high stability can be achieved. According to this approach there are also other examples of ligands that avoids C–H stretching vibration modes in the first coordination sphere of the rare-earth ion [73].

The other approach is focused on the reduction of the number of undesired vibronic modes sources with the halogenation of the ligand, i.e. the substitution of H atoms in the aromatic rings with halogens atoms such as fluorine [76][77], chlorine [78] and bromine [79], to eliminate radiationless decay quenching pathways of *f-f* luminescence associated with the close proximity of high-energy C-H, N-H, or O-H oscillators to the luminescent center [80]. Several examples of halogenated ligands are reported [76-78].

2.2.1 Halogenation of 8-hydroxyquinoline in ErQ

As organic ligand, 8-hydroxyquinoline is affected by the emission quenching of IR erbium emission, too. A work has demonstrated the actual structure of the ErQ molecule is trinuclear, i.e. Er_3Q_9, in which the Er ions are fully coordinated by the quinoline molecules, so resonant activation of aromatic C-H vibrations of the ligand by the erbium electronic excitations is inferred to be the only cause of IR luminescence quenching at 1535 nm and to yield the erbium luminescence lifetime of 2.2 μs [64]. Therefore, halogenation of Quinoline is an effective method to enhance the infrared emission of erbium. Many works on partial halogen substitution in quinoline have been published [79]. One of these has analyzed the synthesis process of lanthanide-doped quinolinates from the point of view of the species involved in a single batch of production. Indeed, in literature it is commonly assumed that complexes of 8-hydroxyquinoline with rare earths are tris complexes (i.e. with the metal-to-ligand ratio of 1:3). However, most synthetic methods to obtain rare-earth quinolinates yield a mixture of different species: hydrated tris complexes, tetrakis complexes, and trimers. It is also demonstrated that the most intensely emitting erbium complexes are the tetrakis complexes of the partially halogen substituted 8-hydroxyquinoline ligand [78].

As shown in Fig. 2.21, Quinoline presents two site for substitution of H atoms naturally bound to the carbon atoms at the positions 5 and 7 (Y and X in the figure) of the group, already exploited in former works [78][79].

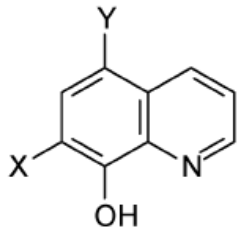

Figure 2.21. Structure of the quinolinate ligand with the positions available for H substitution

An issue must be addressed in the choice of the halogen element. Indeed, as already discussed, the ErQ molecule has been experienced to be difficult to be solvated in common solvents. This is due to the symmetry of the molecule and thus to the high polarity that make it solvable only in similarly polar solvents, such as DMSO. If the symmetry of the molecule is altered by the introduction of big size atoms, the polarity of the molecule can be reduced.

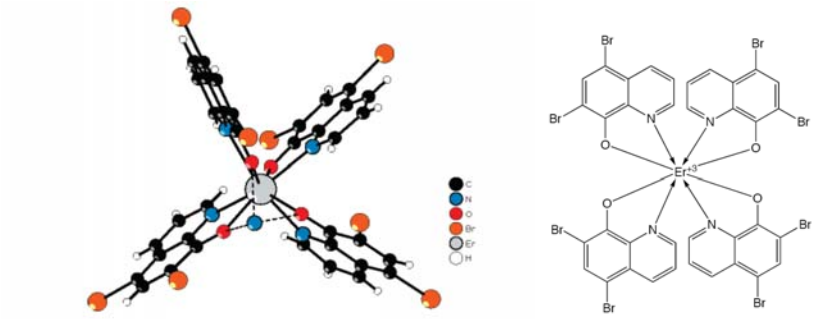

Figure 2.22. Crystal structure and 2D picture of the $Na[Er(Q57Br)_4]$ molecule [78]

Upon these considerations, a new halogenated version of Er-doped quinolinate, Erbium *tetrakis* (5,7-dibromo-8-hydroxyquinoline) Sodium salt ($Na[Er(Q57Br)_4]$), has been synthesized, whose structure is shown in Fig. 2.22. The presence in the molecule of two bromines, that are heavy atoms, allows for the decrease of the polarity. So, this molecule has resulted to be solvable in common solvents such like Chloroform and Toluene. Toluene has been selected as working solvent.

According to what discussed in [78], mass spectrometry measurement has been performed on the compound in order to confirm the presence of the only tetrakis specie, as desired. ESI mass spectrum (see Fig. 2.23) has been obtained by introduction of the sample $Er[C_{26}H_{16}N_4O_4Br_8]Na$ in acetone/methanol solution under negative applied bias. The spectrum shows a peak at 1374 m/z related to the tetrakis compound (1374 m/z) missing of a Sodium ion (24 m/z) that is detached during the solvation. The molecular weight of the tetrakis compound is 1398,02 m/z, so the measure has confirmed the purity of the synthesis. The secondary peak at 303.25 m/z is related to a single ligand group detached from the molecule. Indeed, the ligand group has a negative charge, so it can be observed with the negative bias conditions, whereas the rest of the molecule has a neutral charge, so it cannot be detected by the instruments, as well as the sodium ion that has a positive charge.

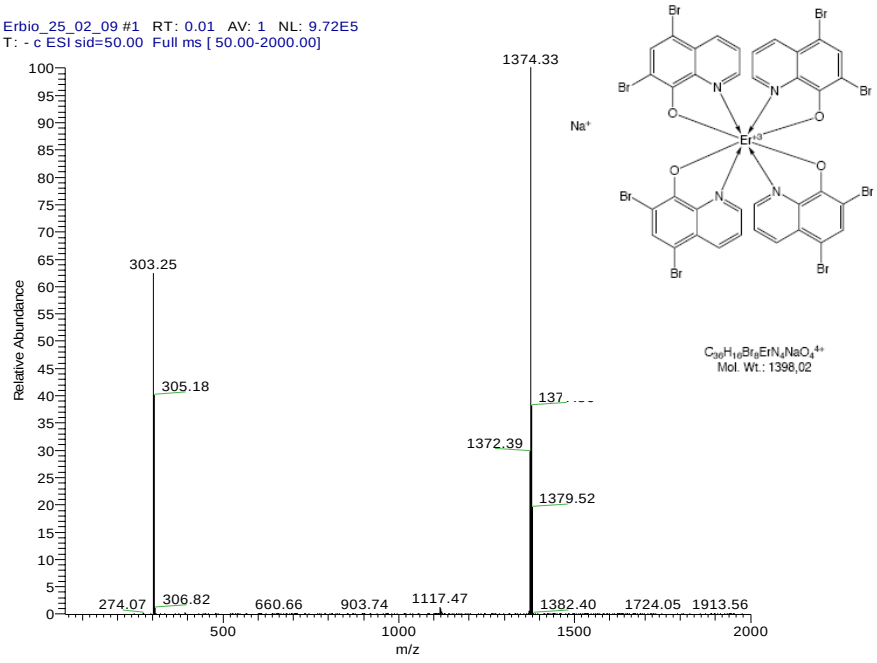

Figure 2.23. ESI mass spectrum of $Na[Er(Q57Br)_4]$

Absorption exhibited by the Toluene based solution (see Fig. 2.24), with a concentration of 2.5 wt. %, shows a red-shifted peak at 402 nm with respect to the hydrogenated Quinoline whose absorption has a peak at 380 nm.

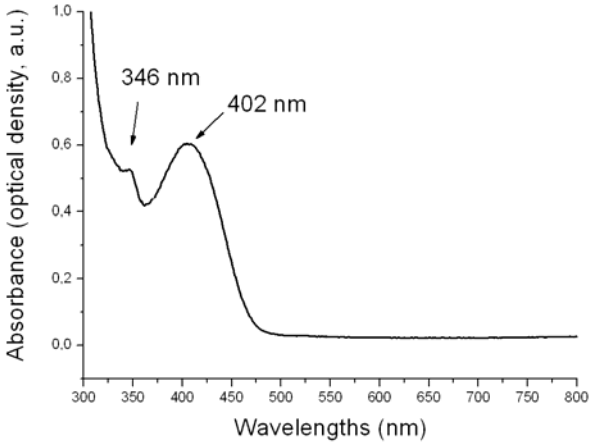

Fig 2.24. Absorption spectrum of Na[Er(Q57Br)$_4$] solution in Toluene (2.5 wt.%)

Visible characterization on the powder (see Fig. 2.25) showed a low-intense broad band superimposed on a self-absorption at 520 nm already observed in ErQ [73]. This band may be ascribed to the quinoline ligands excited singlet states and suggests the existence of an efficient energy transfer path between the ligands and the Er^{3+} ions confirmed by the absence of the triplet emission at 600 nm.

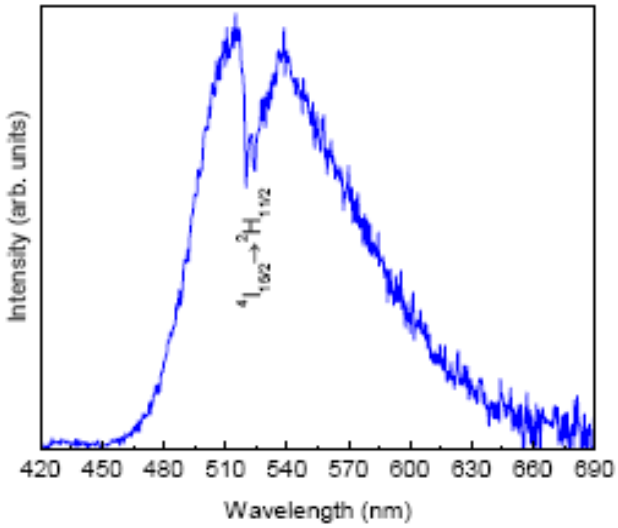

Fig. 2.25. Visible emission of Na[Er(Q57Br)$_4$] powder

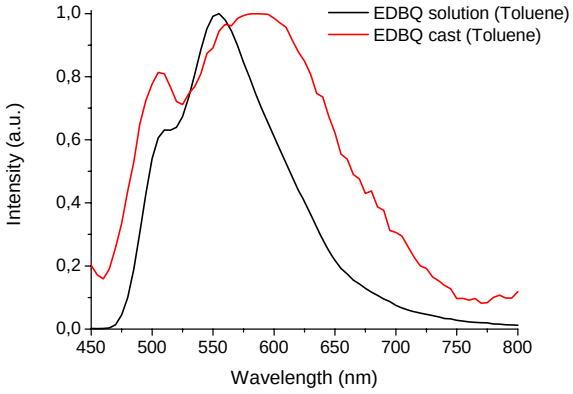

Fig. 2.26. Visible emission of Na[Er(Q57Br)$_4$] solution (Toluene 2.5 wt.%) and the related drop cast film

Visible emission observed on solution and drop cast film (see Fig. 2.26) presents a further primary peak at 555 nm and 585 nm, respectively. This can be related to some kind of interaction with Toluene or to the triplet emission of the ligand, resulting in a less effective transfer from the ligand to the resonant energy manifold in the erbium ion.

Spin-coating deposition of the solution has resulted to be effective with the traditional method, without need of heat sources as for ErQ, as expected from Toluene-based solutions. The spin-coating process has been calibrated for a solution of 2.5 weight %.

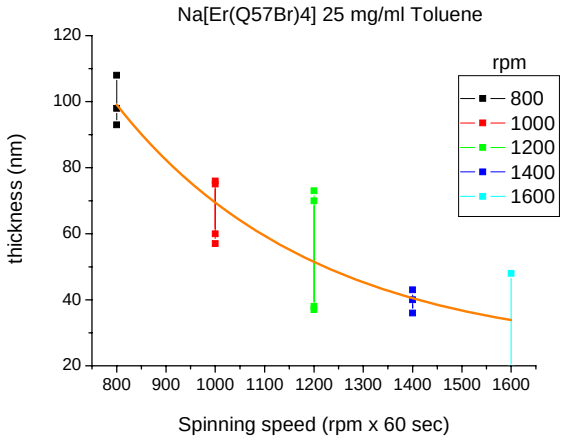

Fig. 2.27. Calibration of spin-coating process for Na[Er(Q57Br)$_4$]

Infrared luminescence observed on spin-coated 60 nm-thick film is shown in Fig. 2.28 with the expected peak at 1530 nm related to the $^4I_{13/2} \rightarrow {}^4I_{15/2}$ transition. The FWHM is 80 nm, with the spectral width ranging from 1485 nm to 1565 nm.

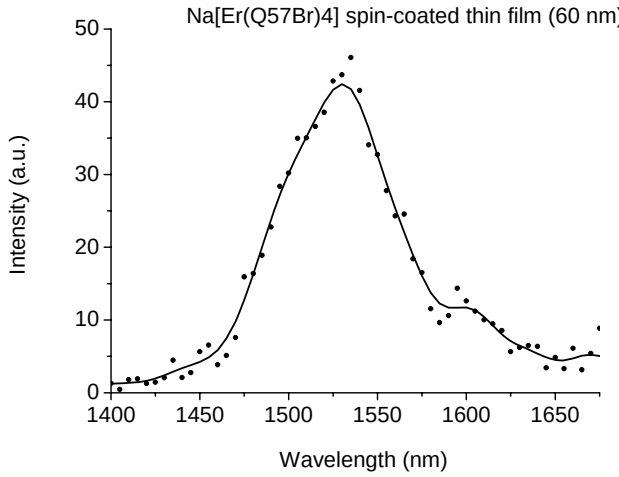

Fig. 2.28 Infrared luminescence of Na[Er(Q57Br)4] spin-coated thin film (60 nm)

Comparison of the infrared luminescence from solution, cast film and spin-coated thin film results in the same behavior, as expected.

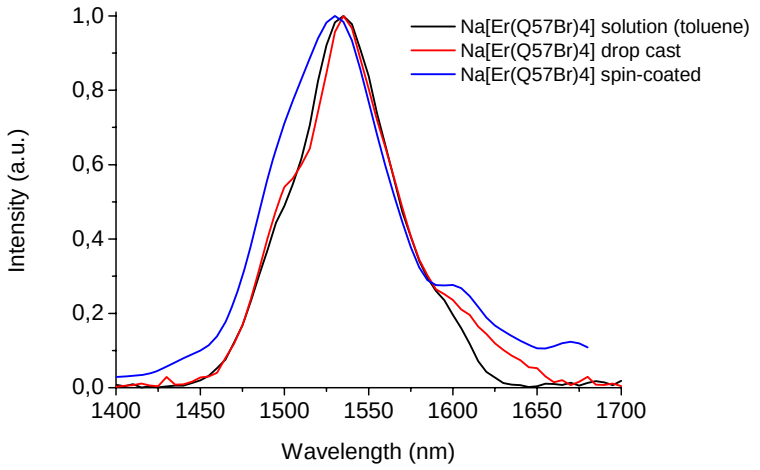

Figure 2.29. Infrared luminescence of Na[Er(Q57Br)4] spin-coated thin film (60 nm), Na[Er(Q57Br)4] solution in Toluene (2.5% weight) and Na[Er(Q57Br)4] cast film

Residuals form synthesis has been solvated in Toluene and optically characterized to evaluate the eventual availability for a practical application and so the production of the synthesis. However, the IR signal observed on drop cast films has been observed to be 50-fold lower, as shown in figure 2.30.

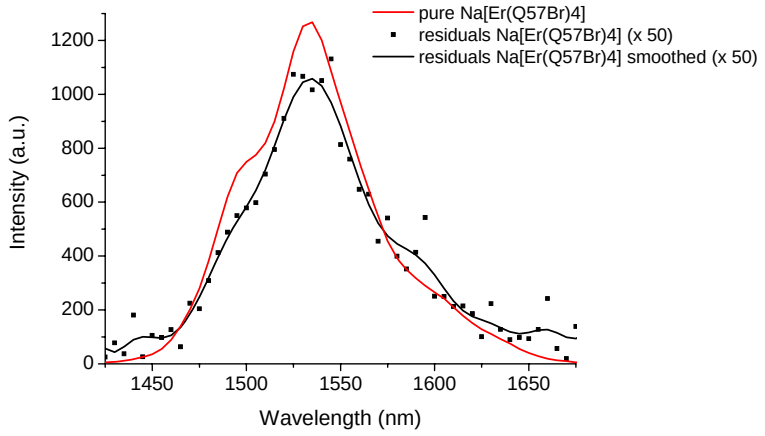

Figure 2.30. IR luminescence of Na[Er(Q57Br)$_4$] and related synthesis residuals drop cast film

Comparison of IR luminescence between Na[Er(Q57Br)$_4$] and ErQ spin-coated films (70 nm thick) is shown in Fig. 2.31, showing a double IR efficiency of the halogenated compound and a substantial correspondence of Er related emission peaks (see Fig. 2.32).

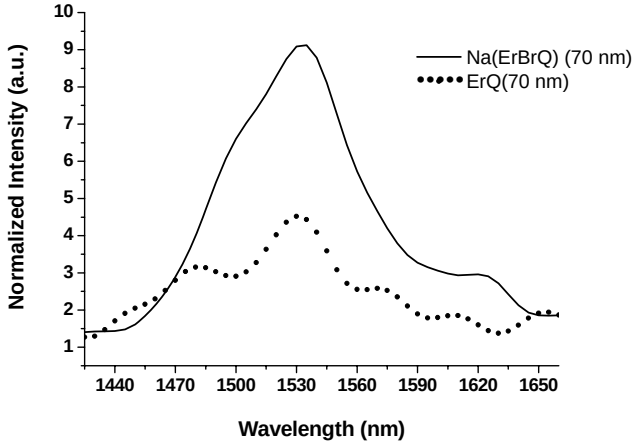

Figure 2.31. Comparison of IR emission efficiency of Na[Er(Q57Br)] and ErQ thin films (100 nm)

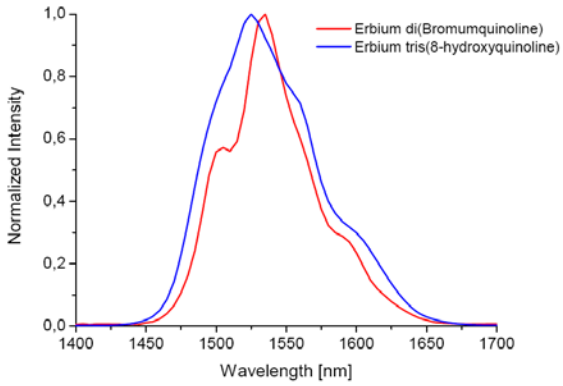

Figure 2.32. Comparison of IR luminescence of $Na[Er(Q57Br)_4]$ and ErQ drop cast films

From a morphological point of view, spin-coating of $Na[Er(Q57Br)_4]$ produces more uniform films than HTSC of ErQ, as it can be observed in figure 2.33, showing optical microscope images of two spin-coated samples of the two materials. As mentioned at the beginning of the chapter, uniformity of thin films is a basic requirement in the processing of organic devices.

So, the synthesis of $Na[Er(Q57Br)_4]$ via halogenation of the quinolinate ligand has produced two results. (1) A double efficiency in the C-band emission of the erbium ion has been reported, due to the reduction of the number of C-H bonds. In addition, (2) an improved processing of the material, in terms of solubility, lower complexity of deposition and higher uniformity of the spin-coated layer, has been achieved.

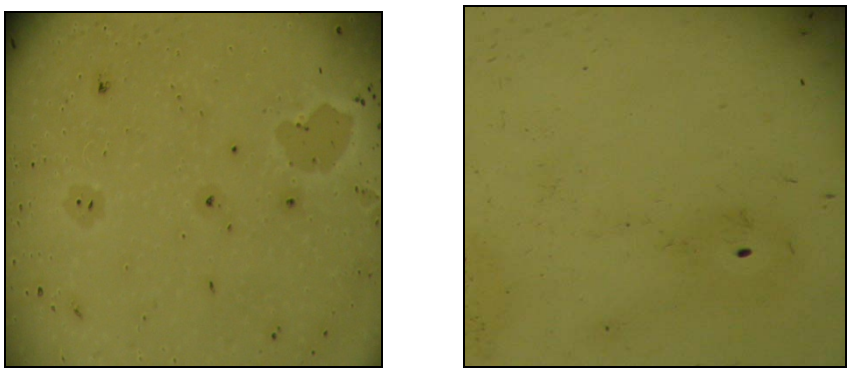

Figure 2.33 Morphology of ErQ (left) and $Na[Er(Q57Br)_4]$ (right) spin-coated thin film, both 100 nm thick, observed at optical microscope (40-fold enlargement)

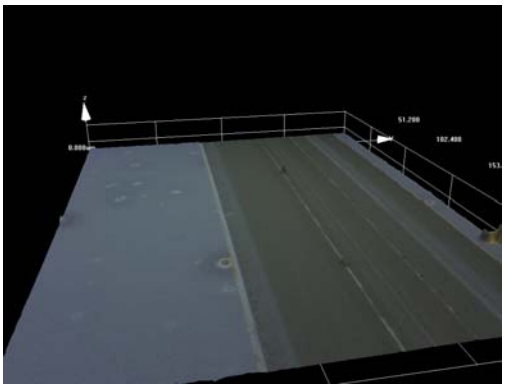

Figure 2.34 Morphology of 100 nm thick Na[Er(Q57Br)] spin-coated thin film: dark zone on the right is due to the scratch needed to to measure the thickness of the film

2.2.2 Fully halogenation of Er-doped tetraphenylporphyrin

Effects of partial and complete halogenation of Er(III) (acetylacetonate) tetraphenylporphyrin [Er(acac)TPP] $Er(TPP)_{acac}$ have been studied, basing on former studies about the full substitution of C-H bonds in the ligand that reported a 10-fold improvement of IR emission in the solution and a 50-fold improvement on the thermally evaporated thin film [81]. Partial substitution has been performed on the external phenyl rings of the molecule with fluorine atoms, resulting in the $Er(acac)(PhF_5)_4TPP$ [77]. Fully halogenation has been achieved by further substitution of the inner C-H bonds by bromine, resulting in the $Er(acac)(PhF_5)_4$ Br_8TPP. The IR emission of the compounds is similar, as expected (see Fig. 2.36).

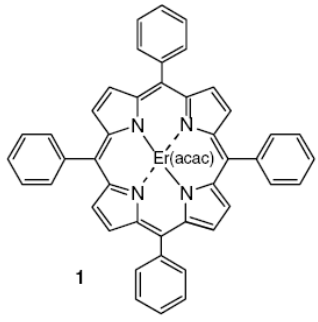

Figure 2.35. Structure of the Er(TPP)acac molecule

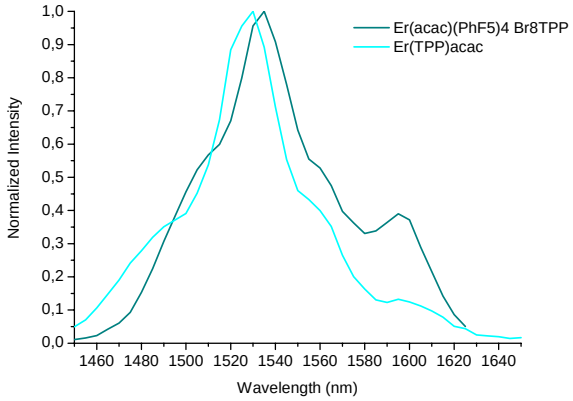

2.36. IR luminescence of non halogenated and fully halogenated ErTPP

Evaluating the enhancement in terms of IR emission, an improvement of 2,5-fold has been observed, much lower than expected [77]. This could be related to the presence of the N atoms in the first coordination sphere of erbium that can be vibration centers resulting in the main cause for quenching of IR emission.

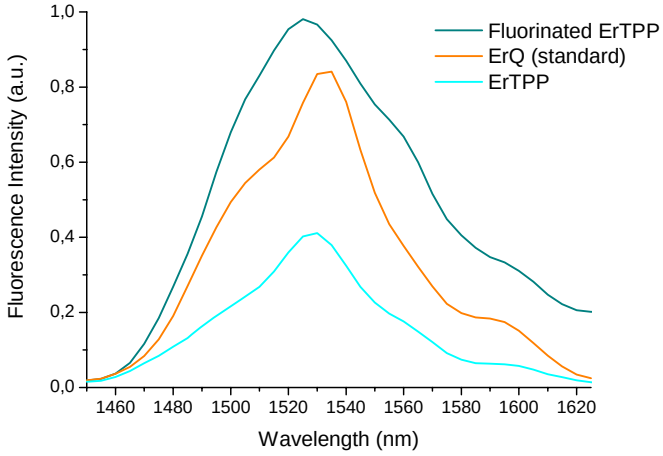

Figure 2.37. Comparison of IR luminescence of ErQ, ErTPP and fluorinated ErTPP solutions

Chapter 3

Organic Light Emitting Diodes for C-band

Opportunity of electrical pumping is one of the unique advantages of organic materials with respect to other amorphous materials for integrated optics such as sol-gels and glasses. Indeed, it would be extremely useful to process an integrated optical device that could be electrically controlled. Such a device could be much cheaper and more compact because no optical pumping would be required. Organic Light Emitting Diodes are basic devices that exploit the semiconducting behavior of some organic compounds to produce luminescence. Since the first OLED has been manufactured [7] much progress has been done on the device structure, optimization of the materials involved and wavelength range of emission. Most of OLEDs research is currently focused on the visible range, because OLEDs represents an alternative technology for imaging and lighting. A big step forward to the OLED technology has been given by the introduction of polymers based LEDs [friend nature], making a huge class of compounds available to be synthesized and functionalized according to the requirements ("tailored" molecules).

For our interest, infrared emitting OLEDs are less popular because no Er-doped polymers have been yet demonstrated. The synthesis of such polymers with good stability is a hard goal to achieve. However, there are some examples in literature of Er-doped small molecules that have been reported to give electroluminescence [62][63][82]. Among them, ErQ is the most popular because of its higher efficiency. Nevertheless, up to now ErQ-based OLEDs have always been

processed by vacuum processing, as discussed in the beginning of the previous chapter.

In this chapter the results of the efforts to process an ErQ-based organic LEDs by spin-coating are reported, with the description of the designed structures and the results coming from the electrical and optical characterization.

3.1 Working principle of an OLED

The working principle of an organic light emitting diode is based on the radiative recombination of opposite charges that interact (exciton) within an organic emitting layer. The organic layer exhibits two molecular orbits, the Lowest Unoccupied Molecular Orbit (LUMO) and the Highest Occupied Molecular Orbit (HOMO), conceptually similar to the energy bands in semiconductors, as shown in figure 3.1. The charges, i.e. electrons and holes, are electrically injected by two metal electrodes, of which one is transparent to allow for light emission outside the device (ITO).

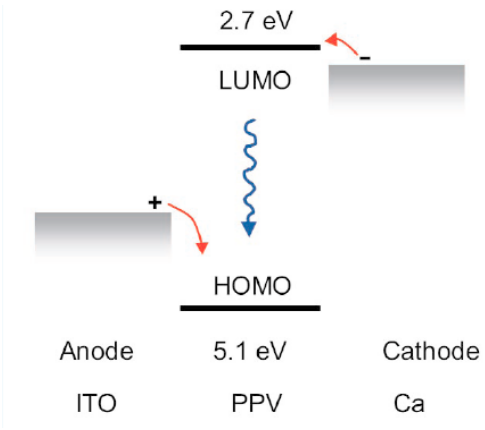

Figure 3.1. Scheme of the working principle of an OLED

The efficiency of external emission η_{ext} in an OLED is ruled by the following expression [83]:

$$\eta_{ext} = \gamma \cdot r_{st} \cdot \eta_{lum} \cdot \eta_{out} = \eta_{\text{int}} \cdot \eta_{out}$$

wherein:

γ is the charge balancing factor related to the different mobility of charge carriers (typically 2 order of magnitude) in the organic film that may result in the recombination at the borders of the emitting layer (less effective radiation);

r_{st} is the singlet to triplet ratio per time unit, related to the multiplicity of the two types of exciton states, singlet and triplet, and their frequency of occurrence; typically a singlet is much more probable than a triplet to radiatively recombine (according to the Pauli's principle), but just a singlet is available per three triplets, so this ratio is set at 25% for most of organics;

η_{lum} is the luminescence efficiency of the radiation generated by the excited state decay calculated on the number of decay transitions, i.e. radiative and non radiative (thermal, vibronic); this value is typically set at 40%;

η_{out} is related to the light that is emitted outside the device; indeed, internal reflections can occur at the interfaces of the different layers, resulting in a source of optical loss;

To maximize the value of the external efficiency multilayer structures are used with the introduction of charge transport materials, in order to achieve a better balancing of the charge transport γ inside the organic layers and a higher probability of recombination inside the active layer.

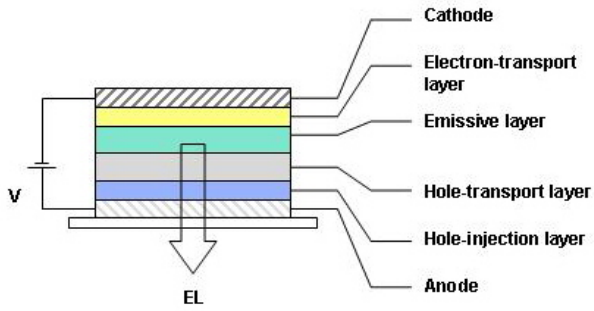

Figure 3.2. Multilayer structure of an OLED [84]

In addition, a careful choice of the materials with the proper HOMO and LUMO, both organics and metals, can allow for minimization of the potential barriers between layers.

3.2 Design of ErQ-based OLEDs

In literature, Er-doped compounds are commonly used as active layers within multilayer structures. Most of Er-doped compounds show a higher mobility for electrons, so they are intrinsically electron transport materials. For such a reason, the different designs of IR-OLEDs involve a hole transporting layer (HTL) to adjust the charge balancing factor. In particular, these strategies may consist on: (1) including an HTL (e.g. NPB) and a hole blocking layer (e.g. BCP) to force holes to recombine inside ErQ thin film as in [85], (2) inheriting basic bi-layer structures [7] with HTL such as TPD, thus exploiting both the electron transporting behavior and the emissive properties of the Er-doped organic as in [63], (3) dispersion of Er-doped compound within an active and electron transporting layer (ETL) as AlQ [7] in order to fully exploit the already developed and optimized structures [61], (4) doping an HTL such as PVK with the Er-compound that acts as electron transporting and emitting material, in order to achieve a good charge balancing with a single layer structure [62].

In this work, two concepts have been followed to design the structures of the device. The first one is based on the structure used for vacuum processed ErQ-based OLED [63], showed in Fig. 3.3, involving a HTL layer such as NPB or TPD and ErQ as emitting layer. A gold thin layer has been introduced at the anode interface to decrease the barrier between ITO and TPD [86].

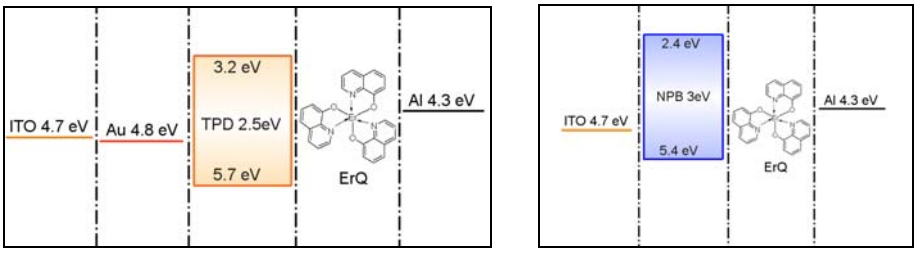

Fig. 3.3 Multilayer structures used for the ErQ-based OLED

The second design, previously never reported, is based on the consideration that usually a relative amount of charges go through the active layer without useful recombination, e.g. recombining in the neighbor transporting layers or at the electrodes. If recombination occurs within a transporting layer that can efficiently emit light in the range of absorption of the active layer, e.g. fro ErQ in the NUV range with efficient tails in the violet, an indirect optical pumping can be exploited in order to partially recover the lost electrical excitation, due to the undesired charge recombination, as optical excitation [56].

The two basic designed structures are shown in Fig. 3.4, involving a blue emitting layer for the transport and ErQ as active layer. The blue emitting layer, Oxadiazole-Carbazole (6,4) (OC), is composed of two moieties, an electron transporting one, Oxadiazole, and a hole transporting one, Carbazole, resulting in a molecule that exhibits the same mobility for holes and electrons. Such a molecule has been demonstrated to give a good blue electroluminescence with a single layer OLED [87]. That is why in the two schemes OC is used in both configuration of HTL and ETL. The good spectral overlap of OC emission with ErQ absorption can be observed in Fig. 3.5.

With respect to the former design concept, it must be remarked that TPD and NPB are blue emitters too, with wide luminescence band centered at 480 nm and 450 nm, respectively, but the emission efficiency is lower than OC, whereas the charge transport feature is peculiar [7][88].

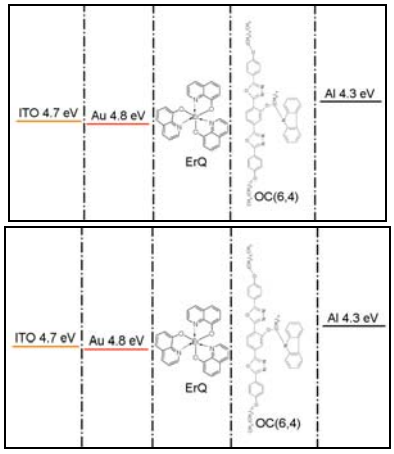

Figure 3.4. Multi-layered structures of the optically/electrically excited ErQ-based OLEDs

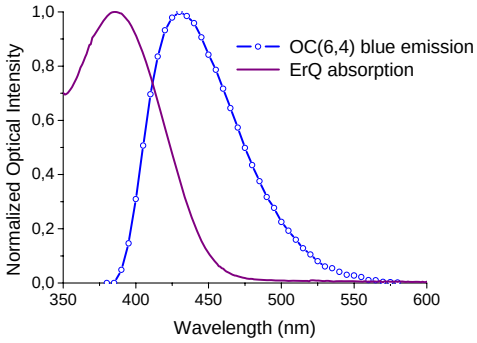

Figure 3.5. Spectral overlap of OC emission and ErQ absorption

It must be noted that an exact characterization of the energy values of ErQ molecular orbits is still missing although several studies [89], so the design of the device structures is not optimized in terms of energy levels. With the introduction of OC, that is a newly lab-synthesized material, the design of the structure is greatly empirical, since energy levels of OC are unknown, too.

3.3 Solution processing and fabrication

One of the aim of this work has been the demonstration of solution-processing as an available fabrication technique for small molecules based IR-OLEDs. Indeed, such a process can provide an appealing alternative for low cost manufacturing, in order to meet the requirements of integrated optics discussed in the first chapter.

To achieve this goal, all the materials selected to be used in the devices have been a subject of study, focusing the experiments on the search for effective solvents to obtain good quality solutions form small molecules and on the calibration and subsequent optimization of the spin-coating deposition, in order to control the final thickness of the coated layer. Two examples of the results produced by this activity are given in Fig. 3.6 and Fig. 3.7, showing calibration of spin-coating deposition for TPD solution (2.5% weight in Chloroform) and OC solution (2.5% in Chlorobenzene), respectively.

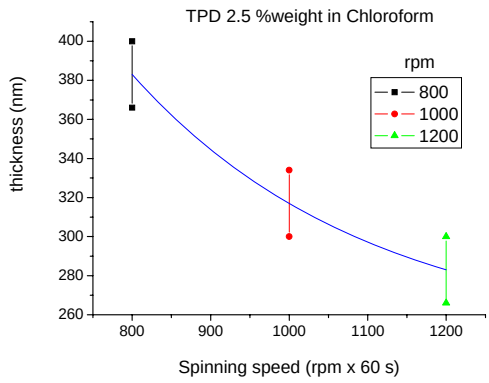

Figure 3.6. Calibration of spin-coating deposition for TPD solution

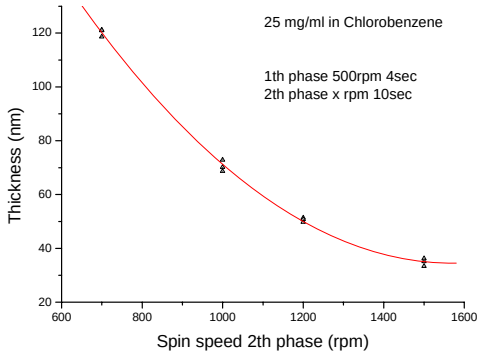

Fig. 3.7. Calibration of spin-coating deposition for OC(6,4) solution

The characteristic values of thickness for the materials used in the devices are described in the following table:

MATERIAL	FUNCTION	SOLVENT	WT. CONCENTRATION	THICKNESS
ErQ	IR emitter	DMSO	4.0 %	60 nm
TPD	Hole transport	Chloroform	2.5 %	40 nm
OC	Blue emitter	Chlorobenzene	2.5 %	35 nm
NPB	Hole transport	Chloroform	2.5 %	40 nm
Gold	Hole injection	-	-	5 nm
Indium Tin Oxide	Anode	-	-	100 nm
Aluminum	Cathode	-	-	100 nm

Table 3.1. Resuming of materials and parameters used in the processed devices

All the devices have been processed under inert atmosphere conditions in a Nitrogen-filled glove-box [MBraun]. The devices have been processed on ITO-coated borosilicate glasses with a 25 Ω/sq sheet resistance [Aldrich]. The golden hole injection layer have been deposited by Argon plasma DC-sputtering [Emitech]. After spin-coating, thermal annealing of organic layers has been performed with a hot-plate. Evaporation of aluminum has been obtained by VTE [Edwards], using a mask to pattern the cathode, resulting in four OLEDs laying on a single substrate. Finally, the devices have been encapsulated by coating the substrate with a glass slide sealed by a thermoplastic film [DuPont] melt at 90 °C on a hot-plate. A picture of the complete device is shown in Fig. 3.8, wherein the blue shade on the glass is related to the OC layer.

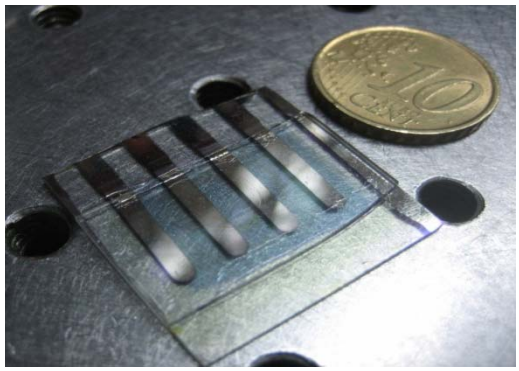

Figure 3.8. Image of the four ErQ-based OLEDs on a single glass substrate

3.4 Characterization

No good results have been observed from the devices designed following the first concept (Anode/HTL/EML/Cathode), both for electrical performance, for which resistive behaviors have been reported, and for optical performances. An explanation of such a failure can be find in the possible detrimental action of DMSO in the ErQ solution on the HTL. Indeed, the high temperatures involved in HTSC can increase the aggression of DMSO over the already coated layers. A proof of that can be provided by graph in Fig. 3.9 that shows a reduction of NPB emission peak after DMSO casting over an NPB spin-coated layer.

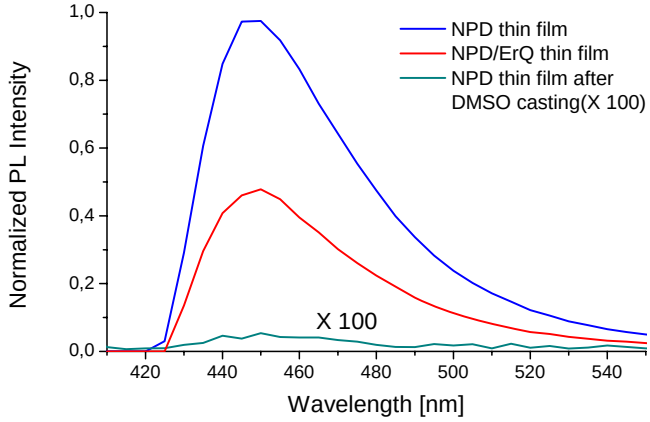

Fig 3.9. Photoluminescence spectra of NPB spin-coated thin films

Instead, the second design concept has provided better results in terms of electrical performances such as diode-like behavior, low threshold voltage, when the OC has been used as ETL, thus avoiding the aggressive action of DMSO.

I- V characteristic showed threshold voltages varying in a range from 4.5 V to 5.5 V, depending on the batch of device process. However, these threshold voltage values are much lower than what reported in [90] wherein the V_{th} was around 15 V. Values of current are strongly variable, depending on the batch of processing. For instance, current values at 6 V can float from 20 mA/cm^2 to 60 mA/cm^2 for nominally equal devices, as it can be observed in Fig. 3.10.

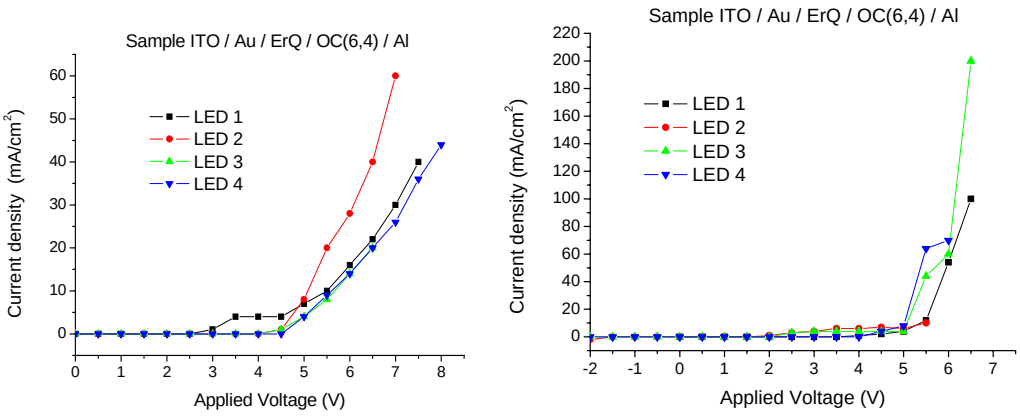

Figure 3.10. I-V characteristics of two ErQ-based OLEDs

Visible electroluminescence detected with a photomultiplier tube is centered at 630 nm. The electroluminescence spectra are confirmed by photoluminescence characterization performed on ErQ solution and ErQ drop cast films shown in Fig. 2.10 and 2.12.

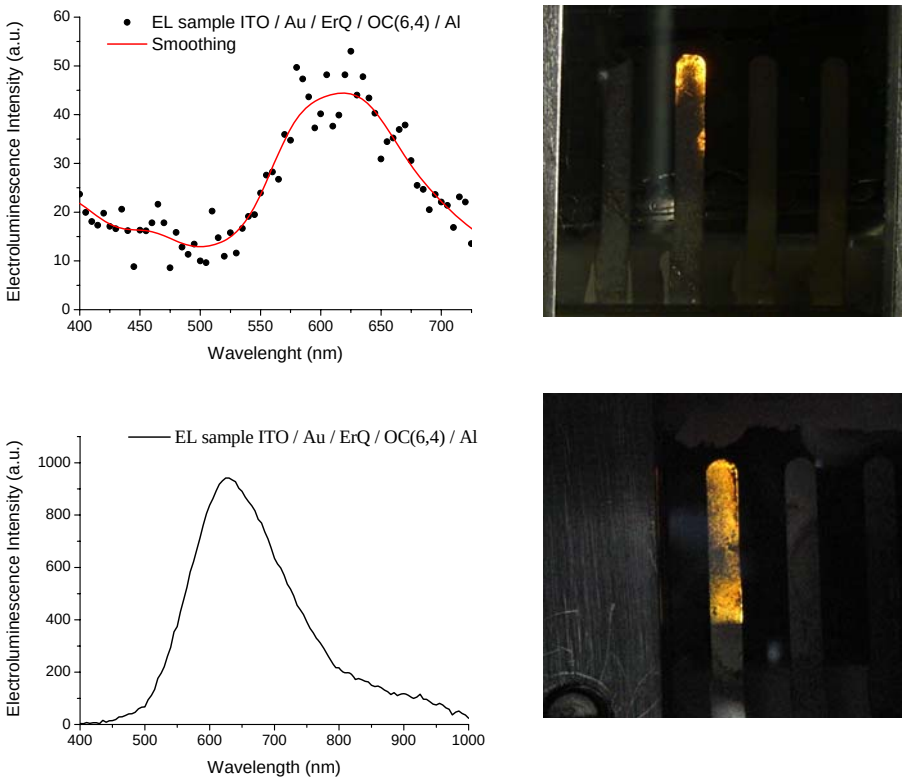

Figure 3.11. Electroluminescence spectra of two nominally equal ErQ-based OLEDs

Infrared electroluminescence is not been detected, maybe due to the high level of noise and low sensitivity of the InGaAs photoreceiver to detect the signal. IR photoluminescence on the device, observed to provide a confirmation of the presence of the ErQ layer also after the deposition of the overlayer, showed the unique erbium related spectrum (see fig. 3.12).

It is reasonable to suppose that IR luminescence has been emitted by the device, even if too low intense to be detected. This thesis is supported by the sensitization scheme of the ErQ molecule. Indeed, the detection of the visible electroluminescence means that the excitation of the singlet state in the Quinoline has been achieved. It is known that energy transfer from singlet to triplet and then to

erbium ion is governed by a statistical law. So the validity of the device structure for charge injection can be confirmed.

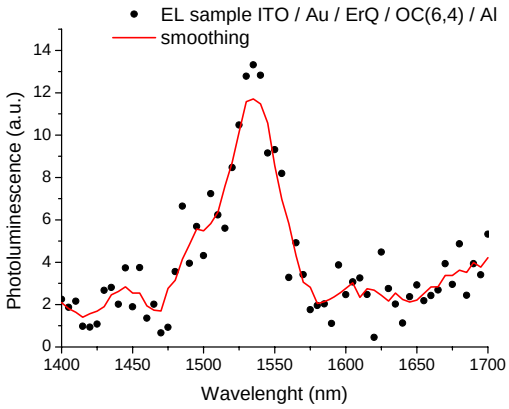

Figure 3.12. IR Photoluminescence of the ErQ-based OLED

Upon the former results, a similar device has been processed, using TPD instead of OC as ETL. This structure is not supported by literature nor theory as TPD is known to be an efficient material for hole transporting rather than for electron transporting. However, good results were obtained with respect to the reverse structure, with good I-V characteristics showing threshold voltages at 5 V and visible electroluminescence observed, even though with lower and less uniform emission with respect to the diodes with OC(6,4).

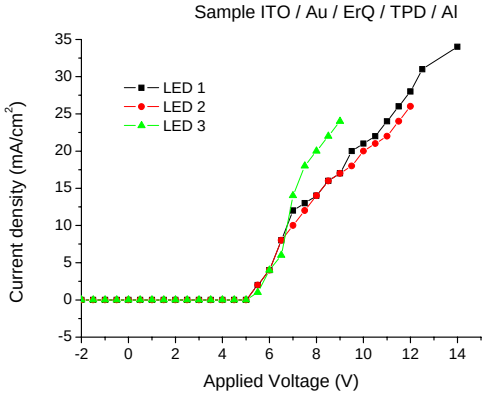

Figure 3.13. I-V characteristic of the ErQ-based OLED

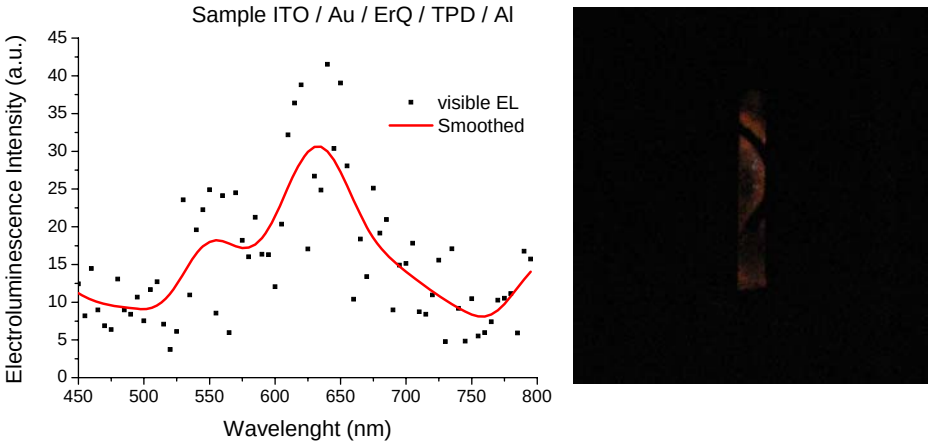

Fig. 3.14 Electroluminescence spectrum of the ErQ-based OLED

In this device the visible luminescence can be related to the radiative decay of the singlet state of the Quinoline, as such as for the previous structures. The noise level is very high, so from the analysis of the former spectra, the 550 nm peak can be considered as part of the singlet emission [63].

In order to verify the presence of the ErQ layer, the infrared photoluminescence of the OLED has been observed. Typical erbium IR emission has been detected, confirming the presence of the ErQ thin film.

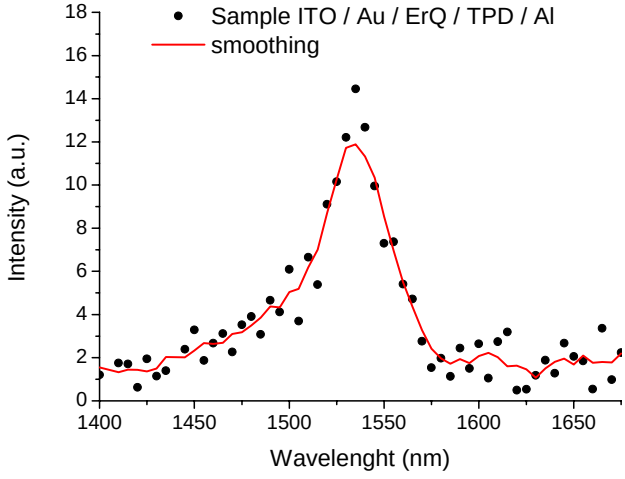

Fig. 3.15 IR Photoluminescence of the ErQ-based OLED

3.5 Na[Er(Q57Br)$_4$] based OLED

Na[Er(Q57Br)$_4$] has been used as active layer in some samples based on the design used in former works. The Na[Er(Q57Br)$_4$] solution based on Toluene is less aggressive, so TPD has been used as HTL. Good I-V characteristic has been observed (see Fig. 3.15), showing high values of current density (60 mA at 11 V) and a threshold voltage set at 8 V. However, although the encapsulation, the devices have shown too low lifetime, resulting in the impossibility to detect the electroluminescence.

The presence of the active layer on the device has been verified repeating the infrared luminescence measurement. The test has confirmed the desired result (see Fig. 3.16), showing also the quality of the thickness control in the OLED processing.

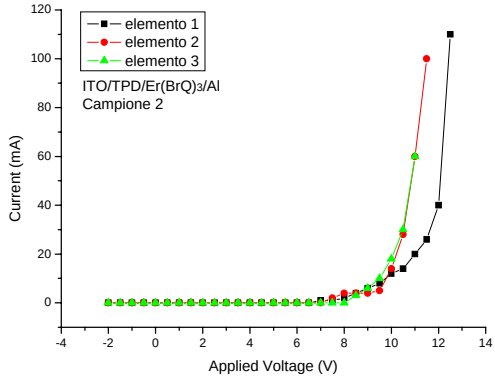

Figure 3.15. I-V characteristics of the Na[Er(Q57Br)$_4$]-based OLEDs

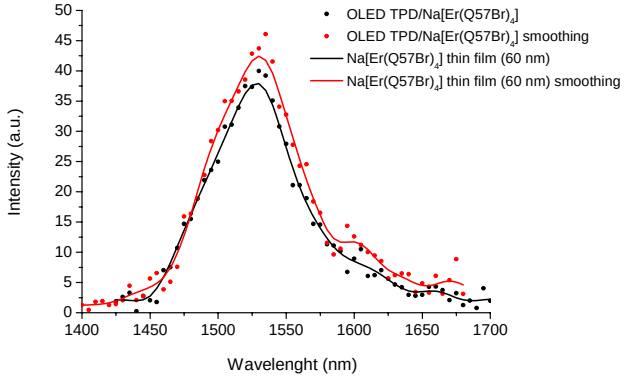

Figure 3.16. IR Photoluminescence of the Na[Er(Q57Br)$_4$] as a thin film and as an active layer in the OLED

Chapter 4

Organic DFB cavities for C-band

C-band lasing represents a challenging issue to be addressed for the development of a complete integrated photonic platform. Indeed, omitting the III-V compounds, laser emission in the C-band requires for Er to be efficiently pumped, but also for an optical resonator to be implemented in order to achieve an efficient amplification. In silicon photonics an impressive breakthrough has been provided by the Er-doped silicon microdisk fabricated at Caltech [91], which light is coupled to with a taper fiber. Other examples of integrated resonators can be found in nano-photonic structures such as erbium activated silica microspheres [92]. Up today, an Er-doped organic laser is still missing, even though a huge progress in OSLs has been made in the last ten years, so that different wavelengths of emission [93-95] and different technologies of design and fabrication [94][96][97] have been demonstrated. Plastic materials have long seemed to be promising as lasing media, largely because of their amorphous structure. Indeed, traditional inorganic semiconductors lasing media such as gallium arsenide have rigid atomic lattices with long-range order. Charge carriers can migrate through them making electric pumping easy. However, the wavelengths of optical transitions in these materials are rigidly fixed, according to the crystalline structure. The rather disordered structure of plastic semiconductors, on the other hand, can be synthesized with widely varying optical and electronic properties. In the past, indeed, organic dyes have been traditionally

used in laser systems to tune the emission through a wide range of wavelengths, that is a typical feature of emission spectra in the organic media [98].

The recent development of Organic Semiconductor Lasers (OSLs) builds on the development of OLEDs, which are now commercially available in displays. Nevertheless, an electrically stimulated OSL has not yet been reported. This is mainly due to three obstacles that must be overcome: 1) the threshold for lasing must be decreased using an architecture containing the electrodes required for charge injection, 2) high carrier injection and high current densities are needed to generate a population inversion and 3) optical losses from charge-induced absorption must be reduced or eliminated [3]. In particular, the second issue is hard to be achieved because of the poor charge-transport characteristics. On the other hand, too thin organic films are not able to provide the gain required for lasing.

Nowadays there is a lack of electrically driven erbium sensitizers based lasers. Indeed, up to now all the resonators have been demonstrated with optical pumping, that is much easier to be driven in order to achieve the population inversion needed for lasing. In addition, the broad absorption spectra and the high absorption cross-sections of the sensitizers make the optical pumping via low cost pump sources, such as LEDs and low cost lasers, possible and thus economically appealing.

In this chapter the first steps on the processing of Er-doped organic DFB cavity are reported. The grating of the cavity has been processed with two different methods: laser interference lithography (LIL) and nano-imprinting lithography (NIL).

4.1 State of the art of organic resonant cavities

In the last decade organic materials have been widely studied to be used as gain material in laser devices, as demonstrated in several works [99-107]. The great potential provided by the organic media can be found in some of their attractive characteristics such as strong optical absorption (a thin film only 100 nm thick can absorb 90% of the light incident on it) [95], high emission quantum yield [108], broad emission bandwidth [98], mechanical flexibility [104], opportunity for electrical pumping [105] and for wavelength tuning on chip [106].

The first demonstrations of the potential of organics for lasing has been given in [99], providing results from a photopumped cuvette containing a MEH-PPV solution. After this work lasing effect has been observed in organic thin films under strong pump excitation, too [95][103][107]. Demonstration of lasing in organic solutions only is not sufficient to validate a material as lasing medium as in the solid

state conjugated organic molecules can interact with their neighbors, leading to the formation of emission quenchers such as dimers, aggregates or excimers. This phenomenon is observed in high concentration solutions, too [108][109].

Lasing media are characterized by the optical gain, meaning that the intensity of light travelling in these materials is amplified by stimulated emission following an exponential growth that is related to the expression:

$$I(z)=I_0 \exp(gz)$$

wherein:

- I(z) is the intensity of light
- I_0 is the intensity of light at z=0
- g is the optical gain coefficient depending on the wavelength

The gain coefficient can be expressed as the product of the stimulated emission cross section, σ, and the population inversion density, N, so $g = \sigma N$. To achieve a good population inversion, that is characterized by a higher number of electrons at the excited states than at the ground state, a multi-level energy system is required, wherein the stimulated emission spectrum does not overlap with the ground state absorption spectrum. From a photophysical point of view, organics behave as four-level systems because structural and vibronic relaxation in the excited states shifts the energy levels [108]. The emission cross section is characteristic of the material. Organic materials can exhibit high luminescence efficiency, up to 60% in thin films and extremely large emission cross section, up to 10^{-15} cm^2[108].

The making of a low threshold organic laser is fundamental to implement a high quality resonant structure in the device [100]. The simplest approach is to design a vertical microcavity, by sandwiching the organic film between a highly reflective and a lower reflectivity mirror [95]. The disadvantage of such a structure is the poor gain of the cavity, as the radiation go through the thickness of the organic thin film, resulting in a very short gain region. On the other hand, implementation of an in-plane Fabry-Perot cavity, even if allows for a huge reduction of the excitation density (from 200 μJ cm^{-2} [5] to 1 μJ cm^{-2} [108]) is not efficient with organics because a low reflectivity can be achieved (10%), due to the lower refractivity of organics (1.5 – 2) [108].

A more effective way to reflect the amplified light in the gain medium and to include a mechanism of wavelength selection is to include a diffraction grating within the laser structure. The grating-based single-mode lasers are classified into two

categories. If the active layer and the grating extend along the whole length of the cavity, the device is known as a distributed feedback (DFB) laser. Instead, if the grating or feedback sections are passive such that the gain region is located in a separate planar gain section, a distributed Bragg reflector (DBR) laser structure is formed [110]. Usually, the net gain difference (or gain margin) between the dominant lasing mode and the most probable side modes is found to be much higher for DFB and DBR structures than for Fabry-Perot lasers. In particular, DFB is considered to be the best candidate for an organic semiconducting laser structure for continuous wave lasing and electrically pumped organic diode lasers. Moreover, the DFB structure can be easily combined with electrical devices such as organic light emitting diodes and light emitting organic transistors. It provides a way to tune the wavelength of the lasing emission through the control of the grating dimension or the film thickness of active layer that controls the effective index of the waveguide mode n_{eff} that can be changed [111].

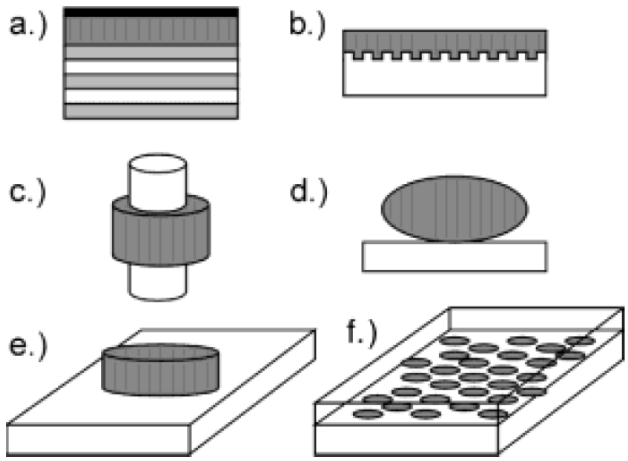

Figure 4.1. Different resonant structures: a.) vertical microcavity, b.) distributed feedback, c.) micro-ring, d.) micro-drop, e.) micro-cylinder, f.) photonic crystal [108]

Typical organic laser structures fabricated in former works are made of vertical emitting micro-cavities with the organic blend sandwiched between two DBR mirrors [112-115], or surface emitting DFB cavities fabricated by holographic lithography [94] or nanoimprinting lithography [116]. Among them, a recent work showed a DFB cavity integrated with a PMMA waveguide providing coupled light to a collection optical fibre [117].

An alternative technology to achieve the resonator is the polymer ring coating fiber acts [118] as guide for the pump signal that efficiently excite the polymeric resonator, providing the typical multimode laser luminescence. The advantages of the microring structures are in the low threshold energies (100 pJ cm^{-2}) and low cost processing (dip-coating) but difficulty they can be used in integrated devices since they do not give off beam of light and because of the large size with respect to the planar devices as the ring diameter is comparable to an optical fiber core (often it is just the fiber core) [108][109].

Towards the low-cost integration, recently a 568 nm emitting organic DFB integrating an InGaN LED as pump has been demonstrated [119]. Threshold has been observed at 144 A current on the short-pulse operating LED pump. This device provides a confirmation of the opportunity of LED pumping as an effective and appealing low cost excitation technology for organic devices, as demonstrated also in [56].

4.2 Design of a DFB cavity for C-band application

Distributed Feed-Back (DFB) cavity has been selected for the design of the resonator as it fits better to the requirements of a waveguided device, such as the compactness and the higher potential for electrical pumping, maintaining the appealing features as like narrow spectral output and single-mode oscillation [110].

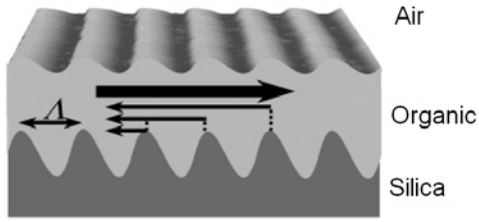

Figure 4.2 Feedback mechanism in an organic DFB structure [109]

The emission of the cavity depends on the parameters of the grating and on the optical properties of the active layer. This dependence is expressed by the Bragg Condition:

$$2\, n_{eff}\, \Lambda = m\, \lambda_{BR}$$

wherein:

- n_{eff} is the effective refractive index of the active material
- Λ is the period (pitch) of the grating
- m is the order of the emitted mode
- λ_{BR} is the wavelength of emission

The refractivity of the ErQ active layer has been calculated with ellipsometry measurements in the infrared range performed on an ErQ evaporated thin film. Evaporation as deposition technique has been forced by the requirement of ellipsometry for high surface uniformity. A refractivity value of 1.63 has been found at 1535 nm, as shown in Fig. 4.3.

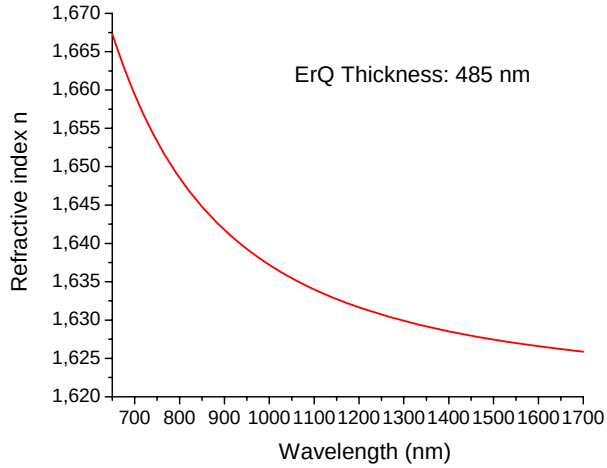

Fig. 4.3. Refractivity of an ErQ thin film measured by IR ellipsometry

Therefore, according to the Bragg condition with the first order of emission (m=1) at 1535 nm, a 472 nm-pitch has been calculated for the DFB cavity. This has been supported by optical field simulations for the cavity based on the Effective Index Method (EIM) [120]. A TM mode has been resulted to be generated in the cavity at the desired wavelength (1530 nm).

Up today, organic DFB cavities have been designed in such a way that the second mode emitted by the grating, that is perpendicular to the grating plan, is

observed [94][116][121]. This results in an easily-to-be-detected surface emission since no edge coupling is required. Such a device is also easier to be processed as the pitch length is double with respect to the first order emission, according to the term Λ/m in the above mentioned Bragg condition, even though the emission intensity is lower than first order grating mode. Nevertheless, in an integrated optical device the surface emitted laser beam is hard to be coupled to a waveguide meeting at the same time the requirements of integrated optics for compactness, low cost and planarity, so an edge emitted cavity, that is purposed for coupling to a fiber or to another waveguided device, has been considered for the design.

The other parameters of the grating, such as the duty cycle and the depth, have been chosen according to former works [94][116]. Typically, the height of the teeth of the grating are in the range of 50 nm - 150 nm, whereas the duty cycle can be varied, apparently with no influence on the performance of the device. However, the development of organic DFBs is just recent, so the influence of grating parameters has not yet been deeply studied.

4.3 Processing

The fabrication of the grating has been performed by mean of two alternative lithographic techniques on a Silica coated Silicon wafer. The active layer has been deposited by thermal evaporation to achieve the high thickness value needed for an efficient emission (thickness > 500 nm). That is why spin-coating has not been involved in the processing.

4.3.1 Grating fabrication

4.3.1.1 Nanoimprinting lithography

There are some works that report on the fabrication of organic DFB structures by NIL [93][104][116]. Nanoimprinting lithography is a quite recent technique that is frequently used for nano-patterning of devices, allowing for the fabrication of high resolution (up to 100 nm), fast and low cost nano-patterns, as demonstrated in several works [122][123]. This also is compatible to organic materials because any detrimental high energy process is used. Typically, a silicon template with the master pattern is pressed over a PMMA

resist coated substrate. There are several alternative variations for NIL, such like soft molding and hot embossing, depending on the method used to transfer the pattern on the sample. In this work, UV embossing has been performed [124].

A Toshiba ST 50 imprinting facilities has been used to imprint a 3.5 cm^2 area on a SiO_2-on-Si wafer. The mold has been fabricated by electron beam deposition. After spin-coating of the UV resist, the sample has been imprinted under UV-exposure. Finally, CF_4 etching has been performed to remove the resist residuals. The actual parameters of the cavity have been measured at a Scanning Electron Microscopy (SEM), resulting in the picture shown in Fig. 4.5, with a pitch higher than expected (500 nm). It can be noted as, after etching, a triangular shaped grating is achieved.

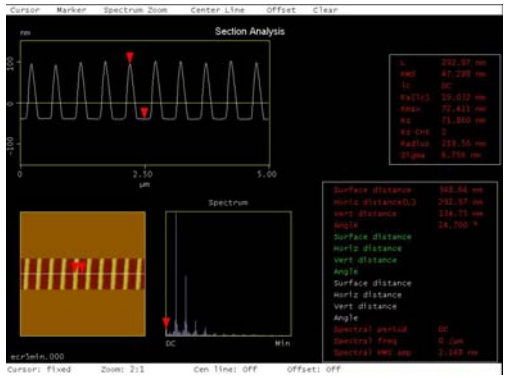

Fig. 4.4. AFM-observed parameters of the imprinted grating

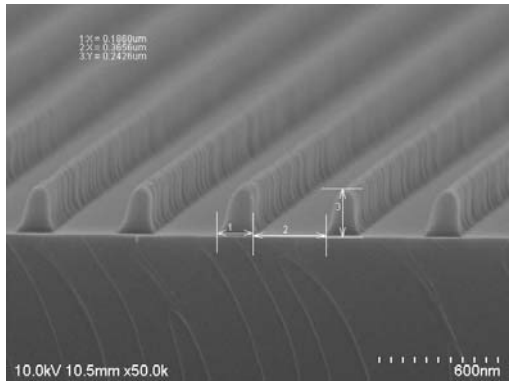

Fig. 4.5 SEM image of the imprinted grating

4.3.1.2 Laser Interference lithography

Laser interference lithography makes use of a high energy coherent source of extreme ultraviolet (EUV) or soft-x-ray radiation. In particular, a coherent tabletop x-ray laser source can be used to achieve unique lithographic features in interference mode, with extremely high resolution [125][126]. This lithographic technique has been successfully tested to realize patterns with sub-micrometer spacing on LiF and PMMA.

For the grating processing, the technique has been used on a poly(methyl-metacrylate) (PMMA) film as a resist. A final semi-cyclic shape grating has resulted, with a diameter of about 50 mm. No etching is involved in the process to remove the resist residuals, so the grating is composed by PMMA teeth with 10 nm depth on the SiO_2/Si substrate. An actual 472 nm pitch has been observed with an Atomic Force Microscopy (AFM).

Figure 4.6. LIL-patterned silica sample: the grating is in the left side (spotted area)

4.3.2 Evaporation of the active layer

Both the types of grating substrates have been coated by ErQ [Aldrich] deposited by vacuum thermal evaporation. Thickness of the layer has been varied between 900 nm and 1000 nm, in order to assure enough active material to observe an amplified emission. Deposition of these so thick layers has resulted from a single batch in a quartz evaporation source. The thickness values have been confirmed by surface profiler measurements. In order to achieve the high purity of deposition, a long desorption step (one hour) has been performed before the ErQ sublimation. Typically, a 2 A/s growth rate has been kept during the process. Figure 4.7 shows the patterned Silica wafer after evaporation of the organic material.

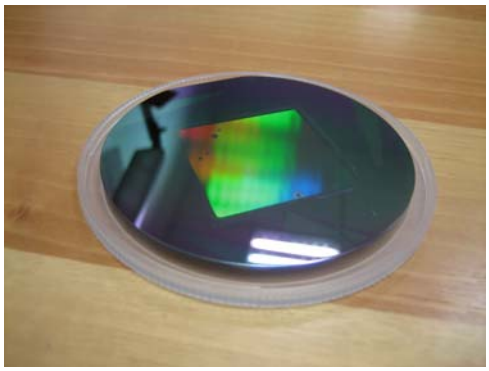

Figure 4.7. ErQ-coated NIL patterned silica wafer

4.4 Characterization

The samples have been characterized with the set-up described in the appendix. Several measurements configurations have been tried to efficiently detect the IR signal. The most used are the perpendicular configuration, with the collection fiber positioned over the sample in order to detect scattered emission from the grating, and the edge configuration, with the collection fiber aligned to border of the pumped grating.

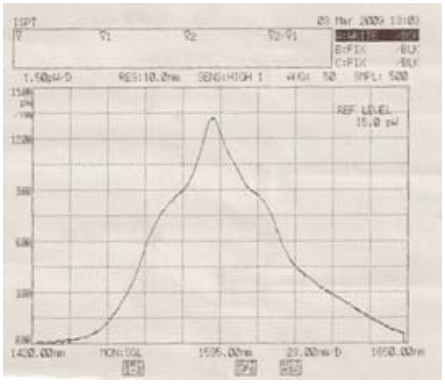

Fig. 4.8 Spontaneous emission of the ErQ-coated grating

The samples processed by NIL have been affected by a mismatch between the optimum designed and the actual pitch observed on the grating after imprinting, resulting in a 1600 nm-centered transmission window. This may represent a cause of

low efficiency of the emission observed. Typical incoherent erbium luminescence, showed in Fig. 4.8, has been detected in the perpendicular configuration.

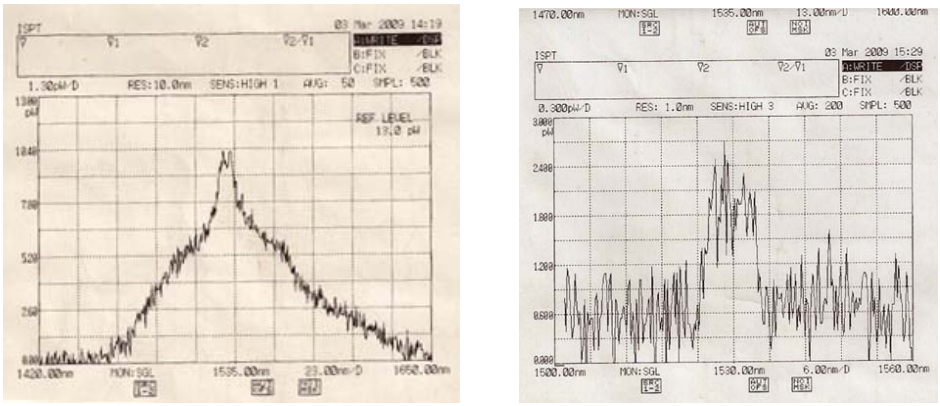

Figure 4.9. Gain narrowing effect on the edge emitted radiation in the NIL cavity

In the edge configuration, the luminescence has been characterized by a 12 nm narrow spectrum at 1530 nm observed both inside and outside the grating region. A possible explanation of such a behavior can be found in [100], that reports the gain narrowing effect of a polymer slab waveguide. Indeed, when the photoluminescent organic has a higher index of refraction than the surrounding media, as it is in this case with the silica substrate having 1.45 refractivity and air cladding having 1 refractivity, an asymmetric waveguide is formed, confining the emitted light which travels along the plane of the organic film. When the pump intensity is high enough for the organic to have net gain, the spontaneously emitted radiation is exponentially amplified by stimulated emission as emitted photons travel through the waveguide. Since the gain is maximal near the peak of the spontaneous emission spectrum, a gain narrowing results [108]. Gain narrowing occurs when the path length exceeds the gain length in the pumped material. Therefore, the gain-narrowed light is guided to the edge of the film or scatters off imperfections in the waveguide, enabling detection in all directions [127]. As a consequence of this discussion, grating has not shown influence on the emission, likely due to the not optimized features for 1530 centered emission, as previously mentioned.

The samples patterned by LIL showed a good peak at 1530 nm. Emission has been detected with an OSA set at 2 nm resolution. The resulting peak is centered at 1530 nm with a 2 nm FWHM, consistent with the resolution. Out of the grating region

just the ErQ spontaneous emission has been observed (see Fig. 4.11), so the peak is not related to the gain narrowing of ASE induced by the waveguiding structure, as in the NIL-patterned DFB, but can be explained by actual laser emission. In addition, this thesis is supported by the power level of the signal that is double than the peak shown in Fig. 4.10 even if resolution, and thus the collected power density (W/nm), is lower (10 nm for the NIL-patterned sample, 2 nm for the LIL-patterned sample).

A comparison of the power level cannot be operated as the fast degradation of the organic material under the laser pumping (50% in 5 minutes) makes any intensity consideration non sensed.

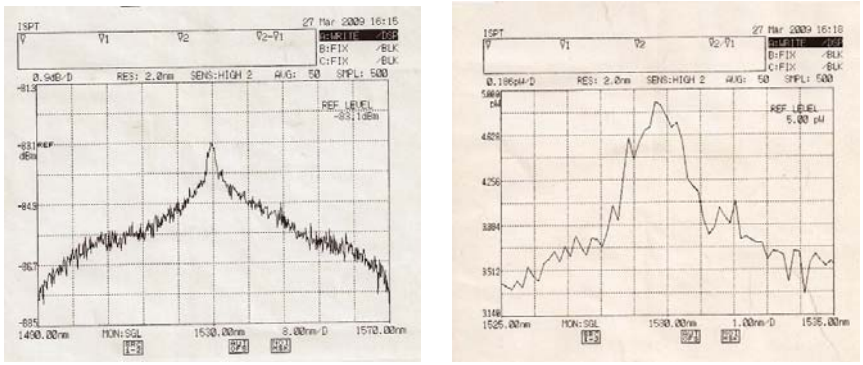

Figure 4.10. Luminescence spectra of the ErQ-coated substrate observed in the LIL-grating

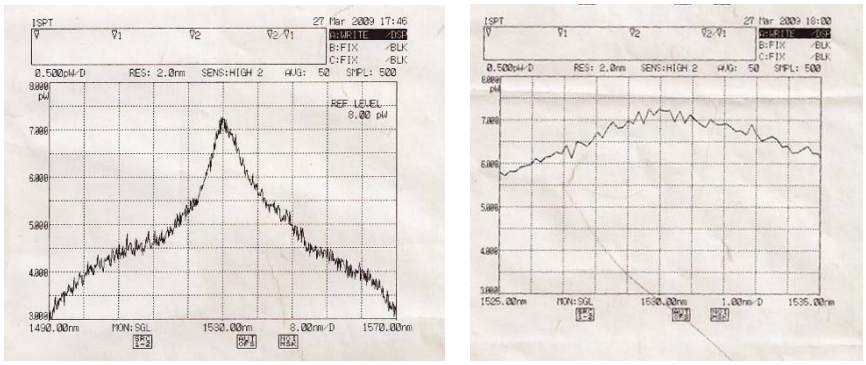

Figure 4.11. Luminescence spectra of the ErQ-coated substrate out of the LIL-grating

Chapter 5

Erbium-doped organic channel waveguides

The optical waveguiding is the basic function for all the integrated photonic circuits. Indeed, as discussed in the chapter 1, light needs to be efficiently confined and made available for coupling to a fibre or to another waveguide device, before any other light processing (generation, amplification, modulation). This requirement represents a limitation on the fabrication of devices because implies the use of step index structures to achieve the light confinement. This affects the choice of the materials. A channel waveguide [128][129] is hard to be processed with a simple and low cost processing technique, since traditional lithographic methods can be detrimental for the organic layers or too expensive. This is the reason why most of the organic waveguides are designed as ribs or slabs [130][131], easier to be processed than a channel waveguide.

In this work an alternative approach has been followed on the design of an optical channel waveguide based on ErQ as active core layer. UV-Photosensitization at the absorption peak of ErQ has been used as low cost technique to induce the refractivity discontinuity, resulting in a channel with the same technological processing of a slab waveguide. It must be noted that the aim of this activity is not to provide the best waveguide for the C-band, but to provide a low cost processing waveguiding structure for the C-band that can efficiently act as platform for integration of the DFB laser reported in the chapter 4.

In this chapter the ellipsometry measurements performed on the photosensitized sample and the results of simulations performed on a possible structure of ErQ waveguide are presented.

5.1 UV-exposure of ErQ thin films

Photosensitization is similar to UV-printing technique, performed in PMMA waveguides. The difference lies in the molecular structure of the materials that are processed: in metacrylates like PMMA the spin-coated solution contains polymer chains which crosslink during the UV-exposure, some polymer solutions also consist of monomers, which polymerize when exposed to UV light [132], UV-exposure instead is mainly applied to sol-gels, in order to tune the refractivity in a range (Δn=0.006) to easily process waveguiding structures with the proper index discontinuity [133].

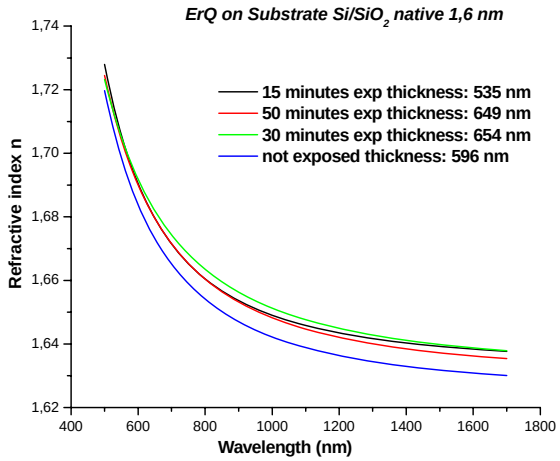

Fig. 5.1. Refractivity of the exposed ErQ coated silica substrates (ellipsometry)

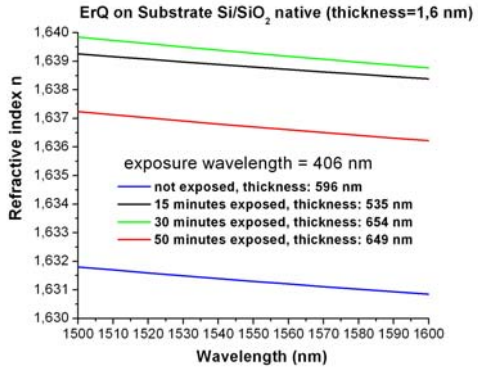

Fig. 5.2. Refractivity of the exposed ErQ coated silica substrates: detail in the C-band

As organic material sensible at UV light, ErQ has been photosensitized at the wavelength usually used to induce the luminescence (λ_{exc} = 406 nm), close to the absorption peak of ErQ, at 380 nm. Four nominally equal samples have been exposed with varying the time of exposure. Ellipsometry measurements performed on the samples (see Fig. 5.1 and Fig. 5.2 with deeper detail in the C-band) showed an increase of the refractivity up to Δn=0.008, in the order of sol-gel tuning range [134].

In addition, a thickness variation has been detected on the four samples by the data interpolation after ellipsometry. This variation has not been confirmed by thickness measurement at the surface profiler.

In order to confirm these data, the refractivity has been measured over three evaporated thin films (1433 nm) by transmittance and reflectance measurement at a spectrophotometer. The exposure time over the samples has been varied with a strong discontinuity, respectively 0 minutes, 50 minutes and 130 minutes, in order to observe the macroscopic phenomena. The results, showed in Fig. 5.3, have provided a similar index discontinuity, around 0.007, even if with slightly different absolute values. Also in this case a variation in the derived thickness of the samples has been observed.

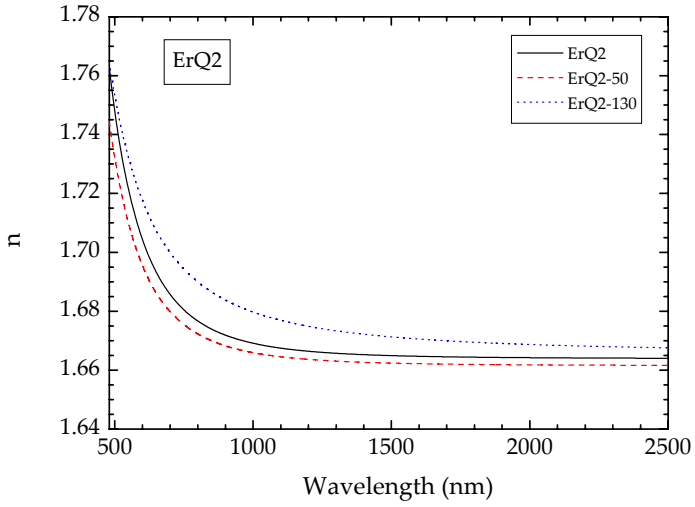

Fig. 5.3. Refractivity of the exposed ErQ-coated silica substrates (transmittance)

5.2 ErQ Channel Waveguide

As mentioned in the beginning of this chapter, typically organic waveguides are fabricated by mean of PMMA or doped PMMA [50]. The most representative application of PMMA is provided by the plastic optical fibres (POF), that have the potential to become the future technology for local area networks because of their low cost simplicity of installation and maintenance, even though the high loss limits their use on short lengths.

Basing on the measurements of refractivity of ErQ thin films and the range of index tuning, a waveguiding structure has been designed using the material involved in the DFB cavity presented in the former chapter, that are 3 μm Silicon Di-oxide on Silicon as substrate and ErQ as active layer.

5.2.1 Design of the waveguide

The waveguide has been designed considering ErQ as active layer, Silica and air as lower and upper cladding layer, respectively. The planar confinement has been studied by supposing photo-patterned ErQ layer as the core because of the higher

refractive index and not UV-exposed ErQ as side cladding layer. The characteristic dimensions of the waveguide are showed in Fig. 5.4: thin film thickness has been varied between 200 nm and 2 μm, the core width has been varied between 2 μm and 5 μm. These dimensions are consistent to similar works found in literature [50]. The characteristic refractive index values are shown in Fig. 5.4.

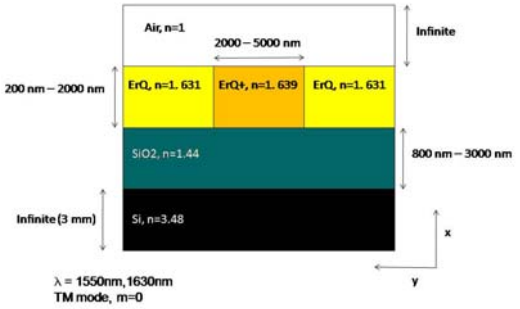

Fig 5.4. Lay-out of the ErQ-based waveguide with typical dimensions

5.2.2 BPM simulations

Crosslight Apsys [135] and Rsoft Beamprop [136] have been used to design the waveguide and study the optical field distribution. These tools use the Effective Index Method (EIM), the most used approach for dielectric waveguides, that is based on the approximation of considering a structure with index discontinuity, such as a channel waveguide, as a slab monolithic waveguide with refractivity defined by an effective refractive index.

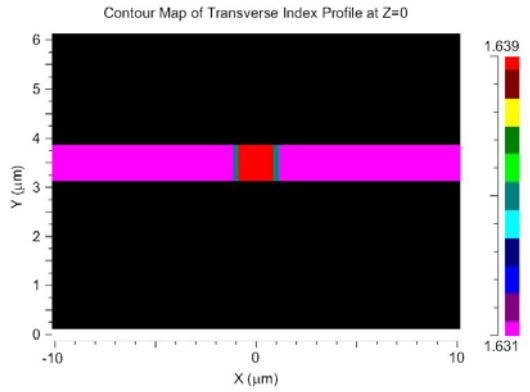

Fig. 5.5. Refractive index distribution at the end facet of the designed waveguide

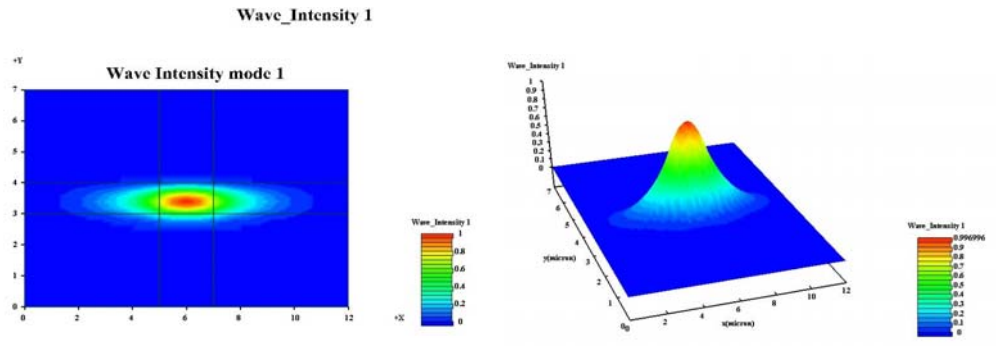

Fig. 5.6. Optical field distribution of the fundamental TM mode (m=0)

Actual refractivity distribution of the waveguide is shown in Fig. 5.5, wherein the index discontinuity in the organic layer has been emphasized in the side scale. The channel features 2 μm width and 1 μm height, according to the actual dimensions of the device cross section shown in the chapter 4. Since TM modes only have been observed to be sensitive to the grating selective action, TM polarization has been selected for simulations.

The optical field distribution shown in Fig. 5.6 is related to the fundamental TM mode with the excitation wavelength set at 1535 nm. It can be observed that a proper light confinement for the fundamental mode has been achieved with a 1 μm thick organic active layer. As expected from the index discontinuity, vertical cut in Fig. 5.7.a shows a strong confinement along the y-axis, whereas horizontal cut shows a weaker confinement along the x-axis (see Fig. 5.7.b).

The higher order modes are not confined, as shown in Fig. 5.8, wherein the highest field intensity is achieved far from the core. For highest order modes (m>7) the radiation is confined inside the silicon wafer that exhibits a high refractivity value (3.48 at 1530 nm).

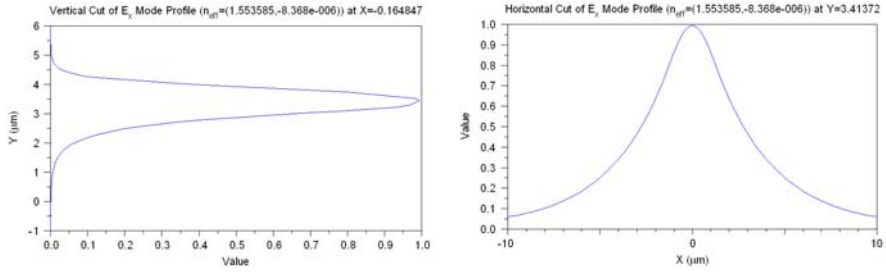

Figure 5.7. a) vertical and b) horizontal cut of the E_x field component in the waveguide

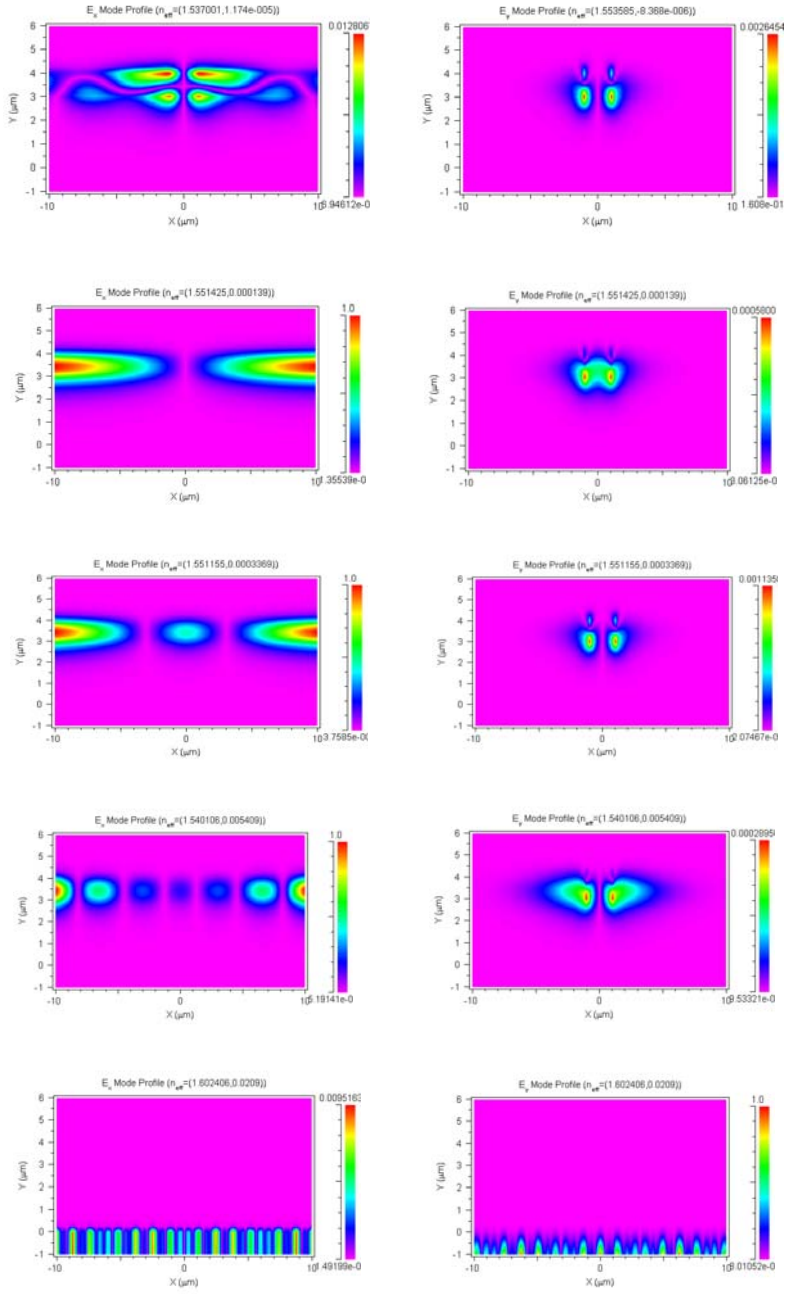

Fig. 5.6. E_x (left) and E_y (right) component of the optical field distribution of the higher order TM modes: respectively, order 1, 2, 3, 7, 8

BPM simulation of the waveguides have been performed considering a Gaussian excitation at the center of the core with 1 μm^2 spot. Fundamental mode has been studied setting the propagation length at 0.8 mm and 2 mm. The related optical profiles at the end facet of the waveguide are shown in Fig. 5.7 and 5.8. A similar behavior can be observed, confirming the good confinement of the radiation.

The transverse cuts of the mode profiles, along the x-axis and the y-axis (see Fig. 5.9), confirms the narrower field distribution and thus the higher light confinement on the vertical cut (width = 1 μm) rather than on the horizontal cut (width = 6 μm), as expected.

Higher order modes have been studied, too, and results on propagation are shown in Fig. 5.10, wherein poor confinement of light can be observed. Therefore, single-mode propagation of the designed DFB structure, assuming UV-photosensitization to write the core in the organic layer, can be assumed.

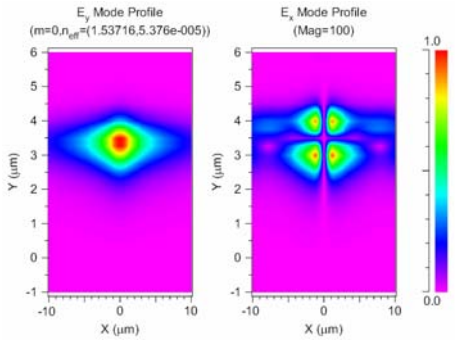

Figure 5.7. Optical profile of the radiation at z = 0.8 mm

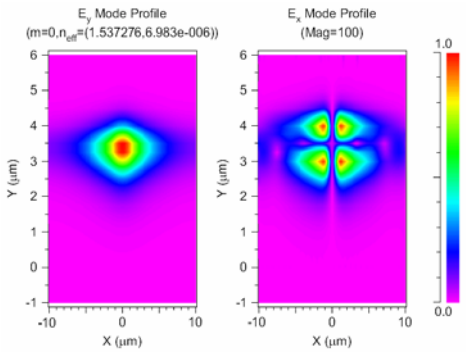

Figure 5.8. Optical profile of the fundamental mode at z = 2 mm

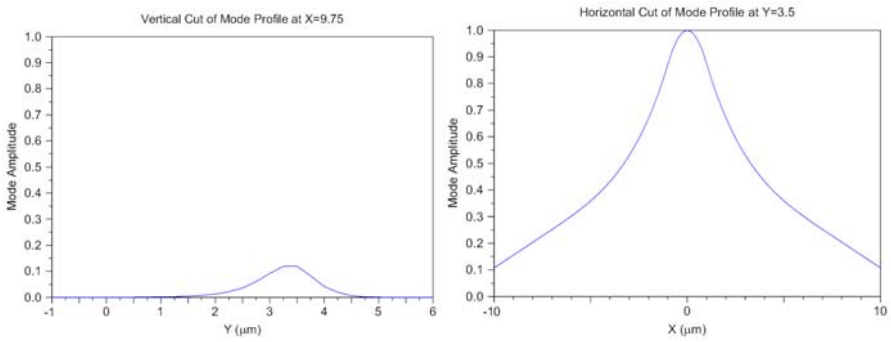

5.9. Vertical (left) and horizontal (right) cut of the fundamental mode profile at the end facet

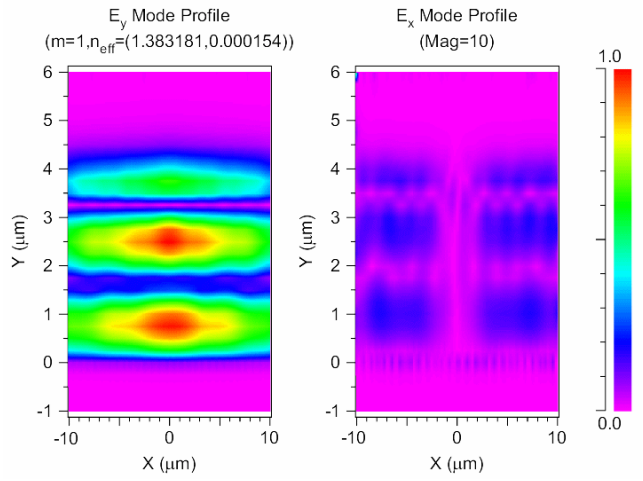

Figure 5.10. Optical profile of the higher order modes (from 1 to 10) at z = 2 mm

Appendix

Luminescence measurement systems

The system used to measure the luminescence is composed of an InGaN laser [Melles Griot], emitting in the violet range at 406 nm, and a halogen lamp [Oriel] as sources, a three blazed monocromator [Oriel Cornerstone] for visible and infrared diffraction, a photomultiplier tube [Newport] and an electrically cooled InGaAs photodiode [Newport] for visible and infrared detection, respectively. Coherent detection system has been used to cut the noise level and improve the signal to noise ratio from the samples. Therefore, a lock-in amplifier [EG&G] connected to the photodetector and to a light chopper, has been used. The system has been aligned and focused by collimation and focusing optics.

In order to demonstrate the opportunity for LED pumping on Er-doped organic thin films, a violet emitting LED [HKTaiyuen] peaking at 402 nm has been used as source.

The system has been controlled by IEEE 488 interface with a purposed routine based on National Instruments Labview software. The lay-out of the measurement system is shown in Fig. A.1.

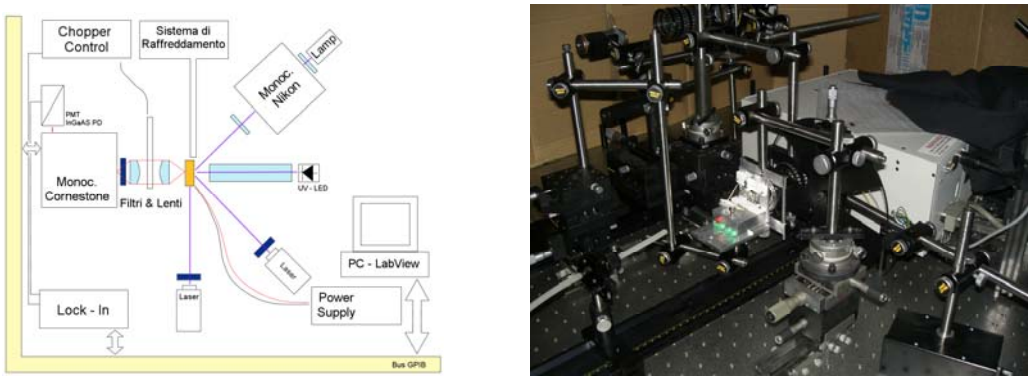

Figure A.1. Lay-out (left) and picture (right) of the system for VIS-IR spectroscopy

The C-band luminescence from the grating samples has been collected by mean of an alternative set-up, involving the same InGaN laser for excitation of the ErQ sample and a large core (400 μm) silica fibre connected to an Optical Spectrum Analyzer (OSA) [ANDO] for light collection. A sphere lens has been used to focus the laser beam over the ErQ sample. Even though the OSA is not purposed to collect the low power signals from organics, it has been used in order to demonstrate the practical use of erbium doped organic materials for photonic applications.

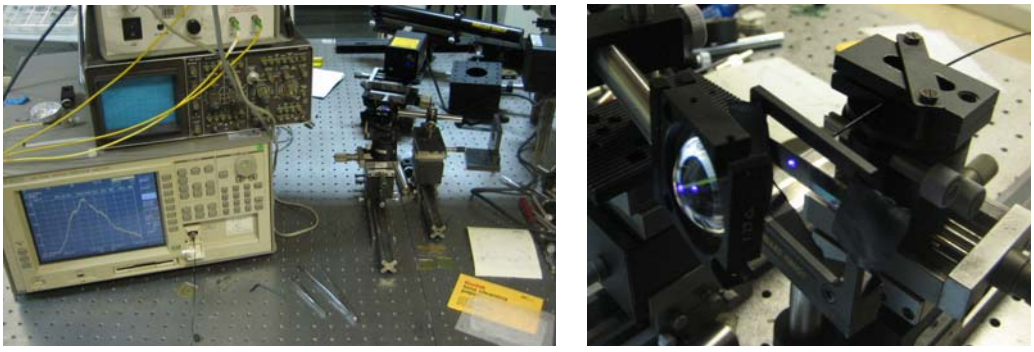

Figure A.2. Large Core Fibre based set-up for infrared spectroscopy on ErQ coated gratings

Conclusions

The aim of this work has been to provide a demonstration of the potential of Er-doped organic compounds for application to integrated optical chips. In particular, an Erbium-doped compound, Erbium *tris*(8-hydroxyquinoline) (ErQ), has been identified as a promising active material for the C-band amplification. The issues for the design and low cost fabrication of an electrically driven organic DFB cavity for integrated optics, still lacking among the optical integrated devices, have been studied.

Low cost processing has been demonstrated by forcing the solution processing of ErQ as deposition technique. A purposed method, high temperature spin-coating, has been developed to efficiently deposit uniform thin films of ErQ.

Electrical pumping has been demonstrated by the processing of an ErQ-based Organic LED. Low threshold and visible luminescence have been observed, confirming the occurred efficient charge injection. Infrared luminescence has not been detected, due to the need for further improvement of charge injection inside the organic layer.

The ErQ-based DFB cavity has been processed by two alternative lithographic techniques, nano-imprinting and laser interference lithography. The last one has allowed for a promising laser peak at 1530 nm with 2 nm FWHM to be observed.

Finally, an ErQ-based channel waveguiding structure has been designed making use of photosensitization of ErQ to induce the right index discontinuity required for planar confinement. Single-mode waveguiding has been demonstrated by beam propagation method simulations. This result enables for the processing of

channel waveguides using simple and low cost fabrication techniques such as spin-coating and photo-patterning.

Therefore, all the technological issues involved in this work have been addressed, showing the potential of Er-doped compounds for actual low cost processing of active integrated photonic devices. The low quantum yield and the fast degradation of the organic materials limit their current use, but improvement of the material with chemical synthesis can be provided by halogenation of the ErQ compound to a Na(ErBrQ) compound, as it has been demonstrated. Higher IR emission efficiency and easier processing of this new compound, never reported in literature, has been observed, showing a way to enhance the performances of the organic active devices.

References

[1] P. Herve, S. Ovadia, “Optical Technologies for Enterprise Networks”, Intel Journal of Technology, Volume 8, Issue 2 (2004)

[2] R.F. Leheny, “Optoelectronic Integration: A Technology for Future Telecommunication Systems”, IEEE Circuits and Device Magazine (1989)

[3] L. Eldada, “The promise of polymers”, *SPIE’s OE Magazine*, (may 2002)

[4] “The Market for Integrated Optical Products: 2001-2005”, http://www.researchandmarkets.com/reports/28429

[5] M.Smit et al., “Photonic integrated circuits: where are the limits?”, *Proc. Integrated Photonics Research and Applications* (2005)

[6] J. Bowers et al., “Integration in 3-D”, *SPIE’s OE Magazine*, (april 2001)

[7] “Polymer TechnologyOverview”, http://www.opticalcrosslinks.com

[8] A. Rahman, “A Review of DWDM “, http://www.arphotonics.net

[9] L. Colace et al., “Ge-on-Si Approaches to the Detection of near-Infrared Light,” *IEEE Journal of Quantum Electronics* 35, 1843−1852 (1999).

[10] H. Rong et al., “A continuous-wave Raman silicon laser”, *Nature* 433, 725-728 (2005)

[11] R. J. Walters, “Silicon Nanocrystals for Silicon Photonics“, PhD Thesis at California Institute of Technology (2007)

[12] M. Paniccia et al., “Silicon Photonics”, *Intel Journal of Technology*, Volume 8, Issue 2 (2004)

[13] A. Pitanti et al., "Er^{3+} coupled to Si nanoclusters rib waveguides", Proc. *5th International Conference on Group IV Photonics GFP* (2008)

[14] I. Izeddin et al., "Energy transfer in Er-doped SiO_2 sensitized with Si nanocrystals", *Physical Review B*, Vol. 78, 3 (2008)

[15] H. Rong et al., "An all-silicon Raman laser", *Nature* 433, 292-294 (2005)

[16] J. E. Bowers et al. , "Hybrid Silicon Evanescent Photonic Integrated Circuit Technology", *Proc. OSA CLEO* (2007)

[17] B.L. Booth et al., "Polyguide(tm) Polymeric Technology for Optical Interconnect Circuits and Components", *Proc. Photonics West Conference*, Vol. 3005, pp. 238-251, (1997)

[18] E.Y.B. Pun et al., "Polymer-based waveguides with low propagation loss and polarization-dependent loss", *Optics & Laser Technology* 37 (2005)

[19] Y. H. Kuo et al., "Low Vπ Optical Polymer Modulator With Novel Poling Strategy", *Proc. OSA Frontiers in Optics* (2005)

[20] D. Ban et al., "Organic–Inorganic Hybrid Optical Upconverter", *IEEE Trans. on Electronic devices*, Vol. 54, 7 (2007)

[21] A. Polman, "Exciting erbium-doped planar optical amplifier materials", *Proc. SPIE* 3942, 2 (2000)

[22] C. Molina et al., "Planar and UV written channel optical waveguides prepared with siloxane–poly(oxyethylene)–zirconia organic–inorganic hybrids. Structure and optical properties", *J. Mater. Chem.*, 15 (2005)

[23] M. Fallahi, "Hybrid Organic-Inorganic for Low-Cost Photonics Integration", *Proc. IEEE ICTON* (2007)

[24] "Metro EDWA™ Datasheet", http://www.teemphotonics.com

[25] S. Pelli, "Erbium-doped silicate glasses for integrated optical amplifiers and lasers", *Journal of Non-Crystalline Solids* 345&346 (2004)

[26] L. Slooff et al., "Optical properties of erbium-doped organic polydentate cage complexes", *J. Appl. Phys.*, Vol. 83, 1 (1998)

[27] A. Polman and F. C. J. M. van Veggel, "Broadband sensitizers for erbium-doped planar optical amplifiers: review", *J. Opt. Soc. Am. B*, Vol. 21, 5 (2004)

[28] J. J. Penninkhof, "Erbium and Thulium doped planar amplifier materials", Master Degree Report at AMOLF-FOM (2002)

[29] L. Slooff et al., "Rare-earth doped polymers for planar optical amplifiers", *J. Appl. Phys.*, Vol. 91, 7 (2002)

[30] E. Desurvire, "Erbium-doped fibre amplifiers: principles and applications", *John Wiley & Sons*, 1994

[31] W.J. Miniscalco, "Erbium-doped glasses for fibre amplifiers at 1500 nm", *J. Lightwave Technol.*, p. 234, 1991

[32] E. Y. B. Pun et al., "Er^{3+}-Yb^{3+} codoped polymeric optical waveguide amplifiers", *Appl. Phys. Lett*., Vol. 84 (2004)

[33] S. Taccheo et al., ”Widely tunable single-frequency erbium–ytterbium phosphate glass laser”, *Appl. Phys. Lett.*, Vol. 68, 19 (1996)

[34] S. Coffa et al., “Temperature dependence and quenching processes of the intra-4f luminescence of Er in crystalline Si,” *Physics Review* B, Vol. 49 (1994)

[35] G. Franzo, “Mechanism and performance of forward and reverse bias electroluminescence at 1.54um from Er-doped Si diodes,” *Journal of Applied Physics*, Vol. 81 (1997)

[36] M. Fujii et al., ‘‘1.54-mm photoluminescence of Er31 doped into SiO2 films containing Si nanocrystals: evidence for energy transfer from Si nanocrystals to Er^{3+},’’ *Appl. Phys. Lett*., Vol. 71 (1997)

[37] F. Iacona et al., “Electroluminescence at 1.54 μm in Er-doped Si nanocluster-based devices”, *Appl. Phys. Lett.,* Vol. 81, 17 (2002)

[38] A. Irrera et al., “Electro-luminescence properties of light emitting devices based on silicon nanocrystals,” *Physica E* 16 (2003)

[39] J. H. Shin, “Si Nanocluster Sensitization of Er-Doped Silica for Optical Amplet Using Top-Pumping Visible LEDs”

[40] J. Broquin et al., “Ion-exchanged integrated devices”, *Proc. SPIE*, Vol. 4277 (2001)

[41] J. Broquin et al., “Ion - exchanged glass DFB Lasers for DWDM”, http://www.teemphotonics.com/assets/files/Technical_Articles/2002-11.pdf

[42] D. L. Veasey et al., “Arrays of distributed-Bragg-reflector waveguide lasers at 1536 nm in Yb/Er codoped phosphate glass”, *Appl. Phys. Lett.*, Vol. 74, 6 (1999)

[43] G. Della Valle et al., “Single-mode and high power waveguide lasers fabricated by ion-exchange”, *Optics Express*, Vol. 16, 16 (2008)

[44] S. Taccheo et al., “Single-frequency glass waveguide lasers”, *Proc. SPIE*, Vol. 7111, 711103 (2008)

[45] J. T. Ahn et al., “Polymer Wavelength Channel Selector Composed of Electrooptic Polymer Switch Array and Two Polymer Arrayed Waveguide Gratings”, *IEEE Photonics Tech.l Lett.*, Vol. 16, 6 (2004)

[46] A. S. M. Supa’at, “A Novel Thermooptic Polymer Switch Based on Directional Coupler Structure”, *Am. J. Applied Sci.,* Vol. 5, 11 (2008)

[47] C. L. Chen, “Fabrication of Polymer Splitter by Micro Hot Embossing Technique”, *Tamkang Journal of Science and Engineering*, Vol. 7, 1 (2004)

[48] L. Eldada et al., “Integrated Multichannel OADM’s Using Polymer Bragg Grating MZI’s”, *IEEE Photonics Tech.l Lett.*, Vol. 10, 10 (1998)

[49] A. Q. Le Quang et al., “Polymer-based materials for amplification in the telecommunication window: Influence of erbium complex concentration on relevant parameters for the elaboration of waveguide amplifiers around 1550 nm”, *Optical Materials*, Vol. 29 (2007)

[50] L. Slooff et al., “Rare-earth doped polymers for planar optical amplifiers”, *J. Appl. Phys.*, Vol. 91, 7 (2002)

[51] O. H. Park et al., "Indirect excitation of Er^{3+} in sol-gel hybrid films doped with an erbium complex", *Appl. Phys. Lett.*, Vol. 82, 17 (2003)

[52] P. Prosposito et al., "Organically modified sol-gel films incorporating an infrared dye", *Thin Solid Films*, Vol. 373 (2000)

[53] B. Alpha et al., *Photochem. and Photobiol.*, Vol 52, 2 (1990)

[54] M. Koppe, "Light Emitting Diodes (LED's) based on Rare Earth Emitters", PhD Thesis at Johannes Kepler Universitat Linz (2002)

[55] F. Artizzu et al., "New Insights on Near-Infrared Emitters Based on Er-quinolinolate Complexes", *Adv. Funct. Mater.* Vol. 17 (2007)

[56] S. Penna, et al., "Near-infrared photoluminescence of erbium tris(8-hydroxyquinoline) spin-coated thin films induced by low coherence light sources", *Appl. Phys. Lett.*, Vol. 91 (2007)

[57] B. S. Harrison et al., "Near-infrared electroluminescence from conjugated polymer/lanthanide porphyrin blends", *Appl. Phys. Lett.*, Vol. 79, 23 (2001)

[58] R. Pizzoferrato et al., "Forster energy transfer from poly(arylene–ethynylene)s to an erbium–porphyrin complex", *Chemical Physics*, Vol. 300 (2004)

[59] Y. Kawamura et al., "Near-Infrared Photoluminescence and Electroluminescence of Neodymium(III), Erbium(III), and Ytterbium(III) Complexes", *Jpn. J. Appl. Phys.*, Vol. 40 (2001)

[60] R. J. Curry et al., "Silicon-based organic light-emitting diode operating at a wavelength of 1.5 μm", *Appl. Phys. Lett.*, Vol. 77, 15 (2000)

[61] W. Q. Zhao et al., "1.54μm Er3+ electroluminescence from an erbium-compound-doped organic light emitting diode with a p-type silicon anode", *J. Phys. D: Appl. Phys.*, Vol. 39 (2006)

[62] R. G. Sun et al., "1.54 mm infrared photoluminescence and electroluminescence from an erbium organic compound", *J. Appl. Phys.*, Vol. 87, 10 (2000)

[63] R. J. Curry and W.P. Gillin, "1.54 um electroluminescence from erbium (III) tris(8-hydroxyquinoline) (ErQ)-based organic light-emitting diodes", *Appl. Phys. Lett.*, Vol. 75, 10 (1999)

[64] F. Artizzu *et al.*, "Structure and Emission Properties of Er_3Q_9 (Q = 8-Quinolinolate)", *Inorganic Chemistry,* Vol. 44, 4 (2005)

[65] C. W. Tang and S. A. Van Slyke, "Organic electroluminescent diodes", *Appl. Phys. Lett.*, Vol. 51 (1987)

[66] J. Thompson *et al.*, "4f energies in an organic-rare earth guest-host system: the rare earth *tris*-8-hydroxyquinolines", *Materials Science and Engineering*, B105 (2003)

[67] H. Suzuki *et al.*, "Organic infrared optical materials and devices based on an organic rare earth complex", *Thin Solid Films,* Vol. 438 –439 (2003)

[68] J. Thompson *et al.*, "Obtaining characteristic 4f-4f luminescence form rare earth organic chelates", *Adv. Funct. Mater.*, Vol. 14, 10 (2004)

[69] H. Suzuki, "Organic light-emitting materials and devices for optical communication technology", *Journal of Photochemistry and Photobiology A: Chemistry*, Vol. 166 (2004)

[70] V. V. N. Ravi Kishore, "On the assignment of the absorption bands in the optical spectrum of Alq_3", *Synthetic Metals*, Vol. 126 (2002)

[71] S.W. Magennis et al., "Time-dependence of erbium(III) tris(8-hydroxyquinolate) near-infrared photoluminescence: implications for organic light-emitting diode efficiency", *Synthetic Metals*, Vol. 138 (2003)

[72] W. P. Gillin and R. J. Curry, "Erbium (III) tris(8-hydroxyquinoline) (ErQ): A potential material for silicon compatible 1.5 mm emitters", *Appl. Phys. Lett.*, Vol. 74, 6 (1999)

[73] R. Van Deun *et al.*, "Strong erbium luminescence in the near-infrared telecommunication window", *Chemical Physics Letters*, Vol. 397 (2004)

[74] S. Moynihan *et al.*, "Optical properties of planar polymer waveguides doped with organo-lanthanide complexes", *Optical Materials*, Vol. 29 (2007)

[75] F. Rizzo *et al.*, "Novel lanthanide complexes for visible and IR emission", *Synthetic Metals*, Vol. 147 (2004)

[76] A. Monguzzi *et al.*, "Novel Er^{3+} Perfluorinated Complexes for Broadband Sensitized Near Infrared Emission", *Chem. Mater.*, Vol. 21 (2009)

[77] S. Pietrantoni *et al.*, "Energy transfer and excitation processes in thin films of rare-earth organic complexes for NIR emission", *Phys. Stat. Sol. (c)*, Vol. 4, 3 (2007)

[78] R. Van Deun *et al.*, "Rare-Earth Quinolinates: Infrared-Emitting Molecular Materials with a Rich Structural Chemistry", *Inorg. Chem.*, Vol. 43 (2004)

[79] R. Van Deun *et al.*, "Halogen substitution as an efficient tool to increase the near-infrared photoluminescence intensity of erbium(III) quinolinates in non-deuterated DMSO", *Phys. Chem. Chem. Phys.*, Vol. 5 (2003)

[80] A. P. Bassett, "Long-Lived Near-Infrared Luminescent Lanthanide Complexes of Imidodiphosphinate "Shell" Ligands", *Inorg. Chem.*, Vol. 44 (2005)

[81] G. Mancino, A.J. Ferguson, A. Beeby, N.J. Long, and T.S. Jones, *J. Am. Chem. Soc.,* Vol. 127, 524 (2005)

[82] Z. Zheng et al., "Optical transition probability of the Er^{3+} ion in $Er(DBM)_3$phen-doped poly(methyl methacrylate)", *Optics Communications*, Vol. 233 (2004)

[83] N. K. Patel *et al.*, "High-Efficiency Organic Light-Emitting Diodes", *IEEE J. on Selected Topics in Quantum Electronics*, Vol. 8, 2 (2002)

[84] http://www.ecu.edu/cs-cas/chem/Shouquan-Huo.cfm

[85] Z. Li *et al.*, "1.54 mm Near-infrared photoluminescent and electroluminescent properties of a new Erbium (III) organic complex", *Organic Electronics*, Vol. 9, (2008)

[86] L. Ke *et al.*, "Au-ITO Anode for Efficient Polymer Light-Emitting Device Operation", *IEEE Photonics Tech. Lett.*, Vol. 17, 3 (2005)

[87] H. C. Neitzert *et al.*, "Blue emitting OLED with oxadiazole/carbazole containing active layer", *Proc. of SPIE*, Vol. 5840 (2005)

[88] C. F. Qiu *et al.*, "Room-temperature ultraviolet emission from an organic light-emitting diode", *Appl. Phys. Lett.*, Vol. 79, 14 (2001)

[89] R. I. R. Blyth *et al.*, "Occupied and unoccupied states of the organic infrared emitters Yb- and Er-*tris*(8-hydroxyquinoline) studied by photoemission and X-ray absorption", *Synthetic Metals,* Vol. 142 (2004)

[90] R. J. Curry *et al.,* "1.5 μm electroluminescence from organic emitting diodes integrated on silicon substrates", *Optical Materials*, Vol. 17 (2001)

[91] D.K. Armani *et al.*, "Ultra-high-Q toroid microcavity on a chip", Nature, Vol. 421, 27 (2003)

[92] G. C. Righini et al., "Integrated optical amplifiers and microspherical lasers based on erbium-doped oxide glasses", Optical Materials 27 (2005)

[93] E. B. Namdas *et* al., "Low Thresholds in Polymer Lasers on Conductive Substrates by Distributed Feedback Nanoimprinting: Progress Toward Electrically Pumped Plastic Lasers", *Adv. Mater.* Vol. 21, (2009)

[94] W. Schneider *et al.*, "Wavelength-tunable organic solid-state distributed-feedback laser", *Applied Physics B – Lasers and Optics*, Vol. 77 (2003)

[95] N. Tessler *et al.*, "Lasing from Conjugated-Polymer Microcavities", *Nature*, Vol. 382, 695 (1996)

[96] G. Kranzelbinder *et al.*, "Optically written solid-state lasers with broadly tunable mode emission based on improved poly (2,5-dialkoxy-phenylene-vinylene)", *Appl. Phys. Lett.*, Vol. 80, 5 (2002)

[97] E. Mele *et al.*, "Polymeric distributed feedback lasers by room-temperature nanoimprint lithography", *Appl. Phys. Lett.*, Vol. 89, (2006)

[98] J. M. Lupton, "Over the rainbow", *Nature*, Vol. 453, 459 (2008)

[99] D. Moses *et al.*, "High Quantum Efficiency Luminescence From A Conducting Polymer In Solution: A Novel Laser Dye", *Appl. Phys. Lett.*, Vol. 60, 26 (1992)

[100] V. G. Kozlov *et al.*, "Laser action in organic semiconductor waveguide and double-heterostructure devices", *Nature*, Vol. 389 (1997)

[101] M. D. McGehee *et al.,* "Semiconducting Polymer Distributed Feedback Lasers", *IEEE Lasers and Electro-Optics Society 1997 Annual Meeting*, Vol.2 (1996)

[102] N. Tessler and R. H. Friend, "Polymer LEDs as Laser Media ?", *Synthetic Metals*, Vol. 102 (1999)

[103] S. V. Frolov *et al.*, "Observation of Superradiance in DOO-PPV films; towards ultrafast lasers", *Synth. Metals*, Vol. 84 (1997)

[104] D. Pisignano *et al.*, "Flexible organic distributed feedback structures by soft lithography", *Synth. Metals*, Vol. 137 (2003)

[105] V. G. Kozlov *et al.*, "Structures for Organic Diode Lasers and Optical Properties of Organic Semiconductors Under Intense Optical and Electrical Excitations", *IEEE J. of Quantum Electronics*, Vol. 36, 1 (2000)

[106] J. Wang *et al.*, "A continuously tunable organic DFB laser", *Microelectronic Engineering*, Vol. 78–79 (2005)

[107] N. Tessler *et al.*, "Lasing characteristics of PPV microcavities", *Synthetic Metals*, Vol. 84 (1997)

[108] M. D. McGehee and A. J. Heeger, "Semiconducting (Conjugated) Polymers as Materials for Solid-State Lasers", *Adv. Mater.*, Vol. 12, 22 (2000)

[109] I. D. W. Samuel and G. A. Turnbull, "Organic Semiconductor Lasers", *Chem. Rev.*, Vol. 107, 4 (2007)

[110] H. Ghafouri-Shiraz, "Distributed Feedback Laser Diodes and Optical Tunable Filters", ed. Wiley (2003)

[111] M. H. Song *et al.*, "Tuning the wavelength of lasing emission in organic semiconducting laser by the orientation of liquid crystalline conjugated polymer", *J. Appl. Phys.*, Vol. 104 (2008)

[112] L. Persano *et al.*, "Low-threshold blue-emitting monolithic polymer vertical cavity surface-emitting lasers", *Appl. Phys. Lett.*, Vol. 89 (2006)

[113] T. W. Lee *et al.*, "Low-threshold lasing in a microcavity of fluorene-based liquid-crystalline polymer blends", *J. Appl. Phys.*, Vol. 93, 3 (2003)

[114] M. De Vittorio *et al.*, "Imprint lithography as a tool for the fabrication of organic-inorganic vertical microcavities", *Proc. 4th IEEE Conference on Nanotechnology* (2004)

[115] M Berggren et al., "Light amplification in organic thin films using cascade energy transfer", *Nature*, Vol. 389 (1997)

[116] P. Del Carro *et al.*, "Near-infrared imprinted distributed feedback lasers", *Appl. Phys. Lett.*, Vol. 89, (2006)

[117] M. Punke *et al.*, "Coupling of Organic Semiconductor Amplified Spontaneous Emission Into Polymeric Single-Mode Waveguides Patterned by Deep-UV Irradiation", *IEEE Photonics Tech. Lett.*, Vol. 19, 2 (2007)

[118] S. X. Dou *et al.*, "Polymer microring lasers with longitudinal optical pumping", *Appl. Phys. Lett.*, Vol. 80, 2 (2002)

[119] Y. Yang *et al.*, "Hybrid optoelectronics: A polymer laser pumped by a nitride light-emitting diode", *Appl. Phys. Lett.*, Vol. 92, 163306 (2008)

[120] Peter Bienstman, CAvity Modelling FRamework, PhD Thesis at Ghent University (2001)

[121] A. Dodabalapur *et al.*, "Resonators and Materials for Organic Lasers Based on Energy Transfer", *IEEE Journal of Selected Topics in Quantum Electronics*, Vol. 4, 1 (1998)

[122] O. J. A. Schueller *et al.*, "Fabrication of glassy carbon microstructures by soft lithography", *Sensors and Actuators*, Vol. A72 (1999)

[123] C. M. Sotomayor Torres *et al.,* "Nanoimprint lithography: an alternative nanofabrication approach", *Materials Science and Engineering C,* Vol. 23 (2003)

[124] M. Nakao *et al.*, "Batch Fabrication of First-Order Grating for DFB Lasers on 3-inch GaAs Substrates by Using UV-Imprint and Chlorine-ICP-RIE Techniques", *IEEE Nanotechnology Materials and Devices Conference (MNDC2008)*, (2008)

[125] A. Ritucci *et al.*, "Interference lithography by a soft x-ray laser beam: Nanopatterning on photoresists", *J. Appl. Phys.*, Vol. 102, (2007)

[126] P. Parisse *et al.*, "Photoluminescence submicrometre spatial modulation of 6,13 pentacenequinone thin films", *J. Phys. D: Appl. Phys.*, Vol. 41 (2008)

[127] M. A. Diaz-Garcia *et al.*, "Plastic lasers: Comparison of gain narrowing with a soluble semiconducting polymer in waveguides and microcavities", *Appl. Phys. Lett.*, Vol. 70, 24 (1997)

[128] M. C. Gather *et al.*, "Embedding Organic Light-Emitting Diodes into Channel Waveguide Structures", *Adv. Mater.*, Vol. 20 (2008)

[129] B. Booth, "Low Loss Channel Waveguides in Polymers", *J. Lightwave Technology*, Vol. 7, 10 (1989)

[130] S. Y Gang *et al.*, "Fabrication of Polymeric Optical Waveguides by B-Staged Bisbenzocyclobutene (BCB)", *Proc ICSE 2004* (2004)

[131] S. J. Bai *et al.*, "Optical attenuation in planar waveguides of unidirectionally oriented copolyester film", *J. Appl. Phys.*, Vol. 79, 12 (1996)

[132] Andrin Stump, "Polymer Based Technology Development for Integrated Optics From the waveguide design to the fibre-pigtailed chip", Université de Neuchâtel 2005

[133] S. Iraj Najafi *et al.*, "Sol-Gel Glass Waveguide and Grating on Silicon"*, J. of Lightwave Tech.*, Vol. 16, 9 (1998)

[134] Crosslight Apsys, licensed to Università degli studi di Roma Tor Vergata, Dip. Ing. Elettronica

[135] RSoft Beamprop, evaluation licensed to Università degli studi di Roma Tor Vergata, Dip. Ing. Elettronica

List of publications

S. Pietrantoni, R. Francini, R. Pizzoferrato, S. Penna, R. Paolesse, F. Mandoj, "Energy transfer and excitation processes in thin films of rare-earth organic complexes for NIR emission", *Physica Status Solidi (c)*, Vol. 4, No. 3, 1048–1051 (2007)

S. Penna, A. Reale, R. Pizzoferrato, G. M. Tosi Beleffi, D. Musella, W. P. Gillin, "Near-infrared photoluminescence of Erbium tris(8-hydroxyquinoline) (ErQ3) spin-coated thin films induced by low coherence light sources", *Applied Physics Letters*, Vol. 91, 021106 (2007)

Published Proceedings

S. Penna, A. Reale, R. Pizzoferrato, D. Musella, G. M. Tosi Beleffi, W. P. Gillin, "Novel Infrared Emitter for Low Cost Optical Devices", *Proceeding on IEEE 9th Int. Conf. on Transparent Optical Networks* (ICTON 2007), Roma (Italy), July 2007

S. Penna, L. Mattiello, G. M. Tosi Beleffi, A. Reale, "Erbium doped organic compounds for integrated optics", *Proceeding on IEEE 10th Int. Conf. on Transparent Optical Networks* (ICTON 2008), Athens (Greece), June 2008

Acknowledgements / Ringraziamenti

At the end of this work, there are many people deserving my personal and professional gratitude. Anyway, before acknowledgements, just some reflections on my PhD. I started almost four years ago with a complete lack of consciousness of what I was gonna study. Indeed, thesis activity left me with a big will to going on research, but little know-how about the subject. Upon this big will, I decided to remain in the university rather than searching for a job, not a usual choice today for Italian engineering students. Working mostly alone, during these 4 years I've experienced bursts of joy and cosmic sadness and, beyond science, I learnt how to organize and manage an activity, from leading students during their thesis period to finding collaborations and access to facilities (not so easy in Italy). I've faced different cultures from mine during abroad periods, and appreciated them as much as mine. This is what I found to be more important of my PhD and unique as experience. That is why I'm satisfied of the scientific work, of the personal growth and mainly of the choice made at the beginning.

I'd like to acknowledge all the guys that contributed with their help and their friendship to my research:

Paolo Prosposito and Cristian Palazzesi from Univesity of Rome Tor Vergata, Dept. of Physics, for the ellipsometry measurements;

Prof. Roberto Pizzoferrato from Univesity of Rome Tor Vergata, Dept. of Mechanical Engineering, for useful discussions

Francesco Michelotti and Francesca Menchini (Sapienza University of Rome, Dept. Of Energetics and ENEA - site of Casaccia, respectively) for transmittance measurements;

Prof. Guido Viscardi from Univeristy of Turin, Dept. of Chemistry, for ESI spectroscopy measurements;

Leonardo Mattiello from Sapienza University of Rome, Dept. Of Chemistry for Engineering, for help and useful collaboration, the most productive chemist I've ever met…high quantity batches from any synthesis!

Prof. William P. Gillin from Queen Mary University of London, Dept. of Chemistry, for the 2004 Christmas present that allowed to me for two years research

People from Universidad de Aveiro, Portugal:

Paulo Andrè from Instituto de Telecomunicacoes (IT), for idea of photosensitization of ErQ and useful discussions;

His wife Rute Sà Ferreira from Dept. Of Physics, for spectroscopy measurements on ErQ;

Antonio Teixeira from IT for fun spent together and financial support;

Carlos Vicente from IT, my companion in the Japanese mission;

Joao, Pedro, Tiago and Ana P. from IT for friendship;

People from ISCOM, Rome:

Franco Curti, for useful discussions and suggestions;

Damiano Musella for support;

Giorgio Maria Tosi Beleffi (GMTB aka Gran Mogol), for fun, friendship, help, support shown in these four years all around the world ();

My companion Davide M. Forin (DMF) for common PhD spent together, even if on completely different subjects;

The freshly mom Silvia Di Bartolo (DIBA) and Gabriele Incerti for common experience and friendship;

People from Fondazione Ugo Bordoni, Rome:

Franco Matera for useful discussions and help;

Luca Rea, my old room-mate at ISCOM, Sergio and Alessandro

People from NICT-Tokyo:

Nakao san, for gratings and for having taught me alternative and more comfortable ways for luminescence detection

Wada san, Sugimoto san, Kataoka san and the great Shinada san

The CHOSERs, my colleagues and friends from Dept. of Electronic Engineering, Optoelectronic group (now CHOSE) at Univ. Rome Tor Vergata, especially:

Prof. Aldo Di Carlo, for providing beer and a future;

Andrea Reale, a friend earlier than a tutor;

Tommy Boy for useful discussions and power moves;

E and R in DYERS (Eleonora and Riccardo) for sincere friendship and all we spent together (I mean time, not money) and we'll going on spending (money, not time);

The grandma Franka (recently the Opter), for friendship and for having been an ever-ready companion for new ideas and experiments;

Peppe Latessa for 5-football

TIBERCADders, that are Ale Pecchia, Fabio Sacconi, Matthias "on the wall", Peppe Romano "sqrt mind solver", Gabo "growling or screaming?"

Valentina Mirruzzo for ready help and friendship

Luigi Salamandra, my alumn (defines me his Senpai) adopted in the framework of the program "Adopt a thesis student", now upgraded to "Adopt a PhD"

My thesis students Elena Iascone, Lucio Cinà, Antonio Cirella (special mention), Silvia Ganci, Charbel Tawk, while following them as tutor I learnt more than what I taught

My girlfriend Siletta "next Irish stew"

My parents and my brother, più che altro per avermi supportato e soprattutto sopportato in questi anni di vita abbastanza disordinati…ma credo ne sia valsa la pena!

Rome, April 23th, 2008 Stefano Penna